AD-A130 822 CAVITY DETECTION AND DELINEATION RESEARCH: REPORT 3 1/1
ACOUSTIC RESONANCE AN..(U) ARMY ENGINEER WATERWAYS
EXPERIMENT STATION VICKSBURG MS GEOTE.. S S COOPER
UNCLASSIFIED MAY 83 WES/TR/GL-83-1 F/G 17/1 NL

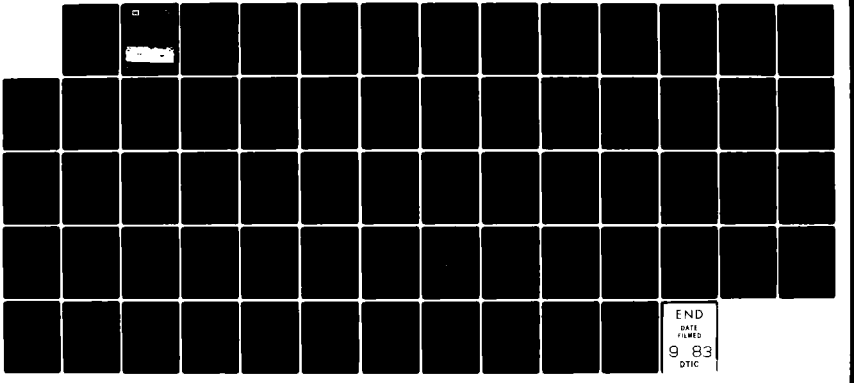

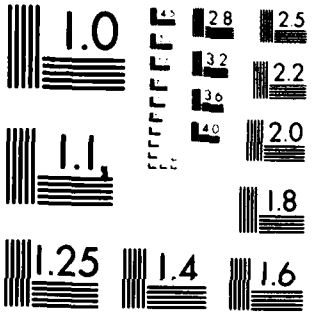

MICROCOPY RESOLUTION TEST CHART
NATIONAL BUREAU OF STANDARDS 1963-A

AD A130 022

TECHNICAL REPORT GL-83-1

CAVITY DETECTION AND DELINEATION RESEARCH

Report 3

ACOUSTIC RESONANCE AND SELF-POTENTIAL APPLICATIONS: MEDFORD CAVE AND MANATEE SPRINGS SITES, FLORIDA

by

Stafford S. Cooper

Geotechnical Laboratory
U. S. Army Engineer Waterways Experiment Station
P. O. Box 631, Vicksburg, Miss. 39180

DTIC
ELECTE
JUL 2 8 1983
A

May 1983

Report 3 of a Series

Approved For Public Release; Distribution Unlimited

Prepared for Office, Chief of Engineers, U. S. Army
Washington, D. C. 20314

Under CWIS Work Unit 31150

DTIC FILE COPY

83 07 27 001

Technical Report GL-83-1

CAVITY DETECTION AND DELINEATION RESEARCH

	Title	Author
Report 1:	Microgravimetric and Magnetic Surveys: Medford Cave Site, Florida	Dwain K. Butler
Report 2:	Seismic Methodology: Medford Cave Site, Florida	Joseph R. Curro, Jr.
Report 3:	Acoustic Resonance and Self-Potential Applications: Medford Cave and Manatee Springs Sites, Florida	Stafford S. Cooper
Report 4:	Microgravimetric Survey: Manatee Springs Site, Florida	Dwain K. Butler, Charlie B. Whitten, Fred L. Smith
Report 5:	Electromagnetic (Radar) Techniques Applied to Cavity Detection	Robert F. Ballard, Jr.

Destroy this report when no longer needed. Do not return it to the originator.

The findings in this report are not to be construed as an official Department of the Army position unless so designated by other authorized documents.

The contents of this report are not to be used for advertising, publication, or promotional purposes. Citation of trade names does not constitute an official endorsement or approval of the use of such commercial products.

Unclassified

SECURITY CLASSIFICATION OF THIS PAGE (When Data Entered)

REPORT DOCUMENTATION PAGE		READ INSTRUCTIONS BEFORE COMPLETING FORM
1. REPORT NUMBER Technical Report GL-83-1	2. GOVT ACCESSION NO. AD-A130 522	3. RECIPIENT'S CATALOG NUMBER
4. TITLE (and Subtitle) CAVITY DETECTION AND DELINEATION RESEARCH: Report 3, ACOUSTIC RESONANCE AND SELF-POTENTIAL APPLICATIONS: MEDFORD CAVE AND MANATEE SPRINGS SITES, FLORIDA		5. TYPE OF REPORT & PERIOD COVERED Report 3 of a series 6. PERFORMING ORG. REPORT NUMBER
7. AUTHOR(s) Stafford S. Cooper		8. CONTRACT OR GRANT NUMBER(s)
9. PERFORMING ORGANIZATION NAME AND ADDRESS U. S. Army Engineer Waterways Experiment Station Geotechnical Laboratory P. O. Box 631, Vicksburg, Miss. 39180		10. PROGRAM ELEMENT, PROJECT, TASK AREA & WORK UNIT NUMBERS CWIS Work Unit 31150
11. CONTROLLING OFFICE NAME AND ADDRESS Office, Chief of Engineers, U. S. Army Washington, D. C. 20314		12. REPORT DATE May 1983 13. NUMBER OF PAGES 60
14. MONITORING AGENCY NAME & ADDRESS(if different from Controlling Office)		15. SECURITY CLASS. (of this report) Unclassified 15a. DECLASSIFICATION/DOWNGRADING SCHEDULE

16. DISTRIBUTION STATEMENT (of this Report)

Approved for public release; distribution unlimited

17. DISTRIBUTION STATEMENT (of the abstract entered in Block 20, if different from Report)

18. SUPPLEMENTARY NOTES

Available from National Technical Information Service, 5285 Port Royal Road, Springfield, Va. 22151

19. KEY WORDS (Continue on reverse side if necessary and identify by block number)

Acoustic resonance
Geophysical investigations
Self-potential
Sonar

20. ABSTRACT (Continue on reverse side if necessary and identify by block number)

In this study three surface geophysical methods were applied to the problem of detecting and delineating subsurface cavities. An acoustic resonance technique was used at the Medford Cave test site in Florida where there are numerous shallow air-filled solution cavities in limestone. Sonar and self-potential (SP) methods were used at the Manatee Springs test site in Florida where water-filled solution cavities are found at a depth of 90 ft below the ground surface.

(Continued)

DD FORM 1 JAN 73 1473 EDITION OF 1 NOV 65 IS OBSOLETE

Unclassified

SECURITY CLASSIFICATION OF THIS PAGE (When Data Entered)

20. Abstract (Continued).

The apparatus and techniques used are described in this report. Evaluations of the methods for detection and delineation of subsurface cavities are presented. Conclusions developed in this study are as follows:

a. The acoustic resonance technique can be reasonably successful in delineating accessible air-filled cavities in limestone if feature dimensions are on the order of a few feet and they are found at depths less than about 20 ft. Features having a high degree of complexity and large (>20 ft) lateral dimensions were not accurately delineated using this technique.

b. The sonar feasibility investigation carried out at Manatee Springs demonstrated that a sonar source can be used to excite large water-filled cavities and the host rock to distances exceeding 200 ft from the source. However, equipment and time limitations restricted the scope of this effort. The data obtained were analyzed but no clear indication of the known cavity feature could be developed. Further study of this method may be warranted.

c. The SP technique used at Manatee Springs did provide useful results. Water flowing in the main solution feature produced readily detectable surface SP anomalies and these data were used to crudely delineate the cavity location in plan view. This result is all that can reasonably be expected of the method considering the complexity of the feature and its depth of burial (90 ft). Neither the above methods nor the self-potential method provide depth determinations.

PREFACE

This study was performed by the U. S. Army Engineer Waterways Experiment Station (WES) for the Office, Chief of Engineers (OCE), U. S. Army, as part of the Materials-Rock Research Program, CWIS Work Unit 31150 entitled "Remote Delineation of Cavities and Discontinuities in Rock." Mr. P. R. Fisher, OCE, was the Technical Monitor, and Dr. D. C. Banks, WES, was the Rock Research Program Manager.

The field work for this study was carried out in August 1979 and October 1980. Individuals contributing to the planning, testing, and analysis phases of the study were Messrs. S. S. Cooper, D. H. Douglas, J. P. Koester, D. E. Yule, and G. W. Deer, Earthquake Engineering and Geophysics Division (EEGD), Geotechnical Laboratory (GL), WES. The project was carried out under the supervision of Dr. A. G. Franklin, Chief, EEGD, and under the general direction of Dr. W. F. Marcuson III, Chief, GL. This report was prepared by Mr. Cooper.

Commanders and Directors of WES during the conduct of the investigation and preparation of this report were COL Nelson P. Conover, CE, and COL Tilford C. Creel, CE. Mr. Fred R. Brown was Technical Director.

DTIC COPY INSPECTED 2

CONTENTS

CONVERSION FACTORS, U. S. CUSTOMARY TO METRIC (SI) UNITS OF MEASUREMENT

U. S. customary units of measurement used in this report can be converted to metric (SI) units as follows:

Multiply	By	To Obtain
feet	0.3048	metres
inches	2.54	centimetres
miles (U. S. statute)	1.609347	kilometres

CAVITY DETECTION AND DELINEATION RESEARCH

ACOUSTIC RESONANCE AND SELF-POTENTIAL APPLICATIONS: MEDFORD CAVE AND MANATEE SPRINGS SITES, FLORIDA

PART I: INTRODUCTION

Background

1. One of the more challenging problems in the geophysical field is the detection and delineation of subsurface cavities. The presence of either naturally developed features such as solution cavities in karstic rock, or man-made tunnels in rock or soil, can be a major concern in a variety of civil and military applications. Some examples include the stability of critical structures such as dams or nuclear power plants founded on karst materials, the erosion of foundation materials by piping, and clandestine tunneling beneath or near military fortifications. Most major construction projects include a program of exploratory borings, some of which may detect cavities through either accident or design. The high cost of drilling often prohibits the use of closely spaced borings to detect and delineate subsurface cavities. Ideally, drilling would be used to confirm anomalies detected by more economical means, possibly geophysical techniques.

Purpose

2. The purpose of this study was to assess the performance of three surface-applied geophysical methods in detecting and delineating known subsurface cavities. Sites with known dry (air-filled) or wet (water-filled) cavities were to be field-tested to determine the sensitivity and resolution of each method used.

Scope

3. This report documents the results of acoustic, sonar, and self-potential (SP) tests carried out at two karst sites in Florida. Medford Cave, a dry site, was tested using the acoustic method. Manatee Springs, a wet site, was tested using sonar and SP methods. Locations of these sites are shown in Figure 1. Field test procedures, the data obtained, and an analysis of results for both sites are presented herein.

PART II: METHODOLOGY

Acoustic Resonance

4. Acoustic resonance techniques for soil studies were first employed by the U. S. Army Engineer Waterways Experiment Station (WES) in the period 1975-76 (Ballard, 1977). This work was directed to identifying shallow man-made tunnels in soil, for military purposes. It was believed that the course of a shallow tunnel in soil could be traced by measuring the ground surface wave amplitudes produced by a loudspeaker placed in the tunnel mouth. In this procedure, the speaker was first tuned to the resonant frequency of the cavity, and wave amplitudes at preselected locations on the ground surface were measured with a very sensitive geophone probe. A schematic of the typical equipment configuration used for an acoustic survey is shown in Figure 2.

5. The acoustic resonance technique met with success in the initial testing over lateral distances of a few hundred feet in soil, and was later used to investigate shallow-buried natural solution channels in rock (Cooper and Bieganousky, 1978). For natural or man-made features at shallow depths, the survey is usually carried out by measuring induced wave amplitudes at the ground surface at points in a predetermined grid pattern. Grid increments equal to about one-half the estimated diameter of the features of interest are typically employed. The general rationale used for interpretation of results is that the maximum amplitude of surface waves emanating from shallow cavities should occur immediately above the cavity roof, and that the absolute magnitude of the induced signal will diminish (through attenuation) with increasing distance from the loudspeaker location.

6. To date, this technique has been applied only at locations where the subsurface cavity was accessible through an opening at the ground surface. However, it would also be possitle to use a high-intensity borehole acoustic source to excite cavities inaccessible by other means. The most recent application of acoustic resonance methods

was at the Medford Cave test site, and results of this study are presented later in this report.

Sonar

7. The acoustic resonance technique previously described may only be used in air-filled cavities. For water-filled cavities, the WES desired to use a similar approach by substituting a sonar source for the acoustic loudspeaker. High-intensity sonar sources suitable for the purpose have been developed by the U. S. Naval Research Laboratory (NRL) at Orlando, Fla. NRL sonar sources have been extensively tested by the U. S. Navy, other Government agencies and private firms, and are documented in the literature (Groves, 1974). These devices are packaged in a variety of sizes to suit specific applications; however, one of the limiting factors is depth of submergence. This limitation did prove to be a problem, as will be discussed.

8. It was desired to test the feasibility of using sonar sources to detect water-filled cavities located at depths up to 100 ft* below the ground surface. Surface delineation of the cavity feature(s) would be accomplished using the same techniques employed in the acoustic resonance study of air-filled cavities. One of the more important questions to be answered was whether the sonar source could deliver sufficient energy to propagate measurable signals for distances of at least several hundred feet in soil and rock. A feasibility study using a sonar source has been conducted at the Manatee Springs test site, and results are presented later in this report.

Self-Potential

9. The movement of pore water in subsurface strata and spatial variations in the chemical composition of the strata and pore fluid can

---

* A table of factors for converting U. S. customary units of measurement to metric (SI) units is presented on page 3.

result in the production of relatively low-level direct current (DC) earth currents, known as self-potentials (SP). The natural steady-state electrical field observed at the ground surface may range in magnitude from a few millivolts to several hundred millivolts or more, depending on local conditions and the method of measurement. For more than 50 years, the surface distribution of the SP field has been used to locate ore bodies, and more recent applications include identification of seepage areas in dams and reservoirs, and geothermal studies (Corwin and Hoover, 1979, and Ogilvy, Ayed, and Bogoslovsky, 1969).

10. For the case of nongeothermal water flowing through underground channels, the flowing fluid forms a double-boundary layer at the channel wall which results in a net negative electrical charge in the surrounding mineral crystals as shown in Figure 3 (Corwin and Hoover, 1979). If the flowing water is fresh (has relatively low salinity), the negative potential may be of sufficient magnitude to produce a significant variation in the surface SP field.

11. The usual procedure for determining SP distribution at the surface is to first place a reference electrode at a relatively large distance from the survey area (usually upstream, if the direction of fluid flow is known with reasonable confidence). A second (survey) electrode is then traversed along a predetermined grid pattern, making repeated DC potential measurements between the reference and survey electrodes. Measurements can be made using a voltmeter with high internal resistance (say, 50 megohms or more) so as to minimize current flow in the circuit. This is necessary to prevent undesirable polarization of the measurement electrodes. Sufficient data are obtained to adequately define the surface SP field, the distribution of which may indicate subsurface cavities. An investigation of this type, conducted at the Manatee Springs test site, is described herein.

PART III: DATA ACQUISITION

Medford Cave Test Site (Dry Site)

12. The Medford Cave test site is located in gently rolling, partly wooded terrain, which has local relief in the site vicinity of about 100 ft. The site area is characterized by a thin (typically 1 to 5 ft thick) layer of sand overlying limestone.

13. Solution activity in the limestones of the area has produced karst topography typified by sinkholes, subsurface cavities, and little or no surface drainage. The top of rock is typically pinnacled, with filled clay pockets between pinnacles. Cap rock at the site is a 3-ft-thick layer of hard molluscan limestone of the Hawthorne formation. This cap is unconformably underlain by limestone of the Ocala formation, which is soft to very soft, friable, and solutioned to form the known portions of the Medford Cave system. The water table at the site is at a depth of about 115 ft below the ground surface.

14. A plan view of the site, showing the general outline of the complex cavity system, profile lines, and borings is presented in Figure 4. Typical cross sections through the main cavity system are shown in Figure 5. A subsurface profile along the 80 north grid line is shown in Figure 6. The cavity outline shown in Figure 4 is only approximate since the complexity of the features precludes complete mapping; outlines of uncertain accuracy are indicated by dashed rather than continuous lines. The original cavity survey was performed by Southwest Research Institute (SwRI) in conjunction with the Florida Department of Transportation. Minor corrections to the plotted outlines were later made by WES.

15. It can be seen from Figures 4 and 5 that the cavity system is typically encountered at depths ranging from 10 to 50 ft below the ground surface, and that the cavities are quite irregular in shape, cross sectional area, and principal direction. This degree of complexity, although probably characteristic of most solution-developed features, is clearly a severe test of resolution for any detection and delineation

method employed. Even so, sufficient control at the site exists to make a meaningful determination of resolution for a range of feature sizes.

16. Considering that features from a few feet to 30 ft or more in width were to be detected, a surface measurement increment of 2.5 ft was adopted as a reasonable choice for the acoustic survey. Three areas selected for survey were known to overlie small, intermediate, and large cavity features and are identified as areas 1, 2, and 3, respectively, in Figure 7. Areas 2 and 3 overlap, and were surveyed using different locations of the loudspeaker within the cavity system. Access to the speaker locations was through the main cavity entrance, in the case of areas 2 and 3, and a secondary cavity opening in area 1. The loudspeaker used was a commercially available unit with a 12-in.-diam bass speaker capable of handling 60 watts root-mean-square (RMS) continuous sine wave electrical input signals. The speaker was excited with steady-state sine waves using a signal generator and a 30-watt RMS rated high fidelity amplifier. After the speaker was placed at the desired location, a frequency sweep was made to determine the acoustic frequency which produced maximum amplitude ground motion (apparent resonance). In the case of survey areas 1, 2, and 3, the apparent resonant frequencies were 116, 108, and 102 Hz, respectively. During each survey the initial frequency and power settings were held constant.

17. As shown in Figure 4, a primary spacing of 20 ft was used in laying out the survey grid. The bulk of the acoustic data was taken at 2.5-ft intervals along the primary grid lines, but some diagonal line and feature tracing measurements were also made where site conditions permitted (parts of the northern half of the survey area are rather heavily wooded, which complicated the measurement process). Acoustic measurements were made with a portable geophone system consisting of three series wired vertical coil elements rigidly housed in a hand-carried spiked probe. A portable battery-powered amplifier and oscilloscope were used to measure the peak-to-peak voltage of the amplified signal from the probe. When surveying, the probe was pushed into the soil until the spike was firmly embedded and then the signal magnitude was read from the oscilloscope with the operator standing still and not

touching the probe. Amplifier gain settings were held constant throughout the surveys (nominally at 1.5 times the geophone output). Approximately 20 sec was required to make a measurement at each station location. A contour plot of acoustic signal magnitude for test area 1, the loudspeaker location, and the estimated (SwRI) and verified (WES) cavity location in this locale are shown in Figure 8. A tabulation of the magnitude of the acoustic signal detected at each measurement location is presented in Table 1. The measured signal magnitudes are expressed in peak-to-peak volts at the resonant frequency of excitation. Since the intent of this survey was to measure relative rather than absolute signal magnitudes, no rigorous calibration of the surface probe geophones was carried out. However, a sensitivity value of 10.0 volts/in./sec is approximately (±30 percent) correct for the gain setting used. Figures 9 and 10 show contour plots of signal magnitude and loudspeaker locations for survey areas 2 and 3, respectively. The acoustic data for area 2 is tabulated in Table 2 and for area 3 in Table 3. All of the acoustic data were obtained by a two-man crew in the period 18-20 August 1979.

Manatee Springs Test Site (Wet Site)

18. The Manatee Springs test site is located approximately 6 miles west of Chiefland, Fla., on the east bank of the Suwanee River, as shown in Figure 1. The site is within the Pamlico marine terrace which, in the site area, consists of a broad shelf of Tertiary limestones covered with a thin veneer of Pleistocene sand. Elevation in the vicinity of the site is 10 to 15 ft, and relief on site is on the order of 3 ft. Erosion of the limestone prior to deposition of the sand had produced an irregular limestone surface, as evidenced by a 13-ft variation in elevation of the top of rock (from borings on site). The coastal terrace is characterized by karst topography which includes sinkholes, vertical piping, poor surface drainage, and solution-developed cavity systems. Large solution features on site are encountered in the

Ocala and Williston limestone units of Eocene age, at depths ranging from 45 ft (spring boil) to 90 ft (main cavity system).

19. A plan view of the Manatee Springs site is shown in Figure 11. In Figure 12, the general outline of the WES-mappped portion of the cavity is shown; dashed outlines indicate areas not mapped for this study. Also shown in Figure 12 is the survey grid used to make surface measurements and the locations of exploratory borings. In the initial phase of developing the test site, it was necessary to locate the subsurface features with greater precision than that afforded by existing maps (Figure 11). Borings S-1 and C-1 were drilled to provide reference points from which more precise measurements of the cavity features could be made. Members of the Cave Divers Section, National Speleogical Society then resurveyed the cavity features of interest so that other boreholes (C-2 through C-5) could be situated to bracket a side tunnel feature for purposes of a different study not reported herein. Boreholes E-1 through E-6 and UL-2 were drilled later to better define areas of interest at the site. From these data and divers' observations, the cross sections shown in Figures 13 and 14 were developed. It should be stressed that the main cavity outlines shown in Figure 12 are correct insofar as major features are concerned, but that the divers reported areas where secondary cavity features are so numerous that the limestone resembles Swiss cheese. However, as in the case of Medford Cave, major accessible features have been mapped in sufficient detail to premit a meaningful test of resolution for the survey methods employed.

20. Sonar and SP investigations at the site were completed in the period 9-15 October 1980 by a three-man WES field crew. The SP survey was conducted by taking measurements with the survey electrode at 10-ft intervals along the E-W grid lines already established. The reference electrode was located in Sue's Spring, approximately 750 ft upstream, as shown in Figure 11. The potential difference between reference and survey electrodes was measured with a commercially available digital volt-ohmmeter having an internal impedance of 1000 megohms. The electrodes used were porous pots of the copper-copper sulfate type,

which were connected to the volt-ohmmeter with multistrand 16 AWG insulated wire. All of the measured SP data are tabulated in Table 4. Figure 15 is a plan view of the SP survey area which shows the survey grid, subsurface cavity outline, and equipotential contour lines developed on 20-mv intervals.

21. In the sonar feasibility study, the sonar source was positioned as shown in Figure 16 using a small boat to suspend the source in the sinkhole identified in Figure 11 as the "Catfish Hotel." This sinkhole communicates with the main cavity system at a depth of about 90 ft below the ground surface. Because of previously mentioned limitations on its depth of submergence (maximum depth = 75 ft), the sonar source could not be placed directly in the main cavity. At depths greater than 75 ft the internal pressure-equalizing system in the device cannot compensate for hydrostatic pressure on the moving diaphragm, causing a drastic decrease in output.

22. A frequency sweep was first performed to determine the discrete frequency at which surface-received signals had maximum amplitude. The sonar source was driven using a tone burst signal generator and an amplifier capable of delivering 250 watts of continuous power. However, the sonar source could accept only 50 watts power input so this excitation level was maintained throughout testing. After determining that 123 Hz was the best signal propagation frequency for this site, the pulse generator was used to automatically pulse the sonar source (1 sec on, 1 sec off) during data acquisition. Since there is always some background seismic noise at any test site, pulsing the sonar signal was a convenient way to differentiate between noise and the signal of interest when weak signals were being received. The peak-to-peak amplitude of surface-arriving sonar pulse was measured using the portable geophone system described in paragraph 17; however, the amplifier gain was increased to yield about 400 volts/in./sec total system output sensitivity in an effort to detect very feeble signals at some locations on site. It had been hoped that naturally occurring water turbelence in the main flow channel might produce measurable signals at the surface; however, background noise surveys indicated that these signals, if

present, were too feeble to detect even with the increased gain settings used. Hence, only sonar pulse data are presented herein. The sonar data are tabulated in Table 5. Results of the sonar feasibility survey are also shown in Figure 17, which is a contour plot of peak-to-peak voltage amplitude of received signals using 1-volt contour intervals.

PART IV: ANALYSIS OF RESULTS

23. Both the acoustic resonance and sonar methods have to date been employed as a means to delineate cavities whose presence is known. Consequently, an evaluation of these methods is properly directed to their ability to delineate cavity features. On the other hand, the self-potential method may be employed to both detect and delineate subsurface cavities, provided they are water-filled, some flow is taking place, and other necessary conditions (such as low salinity pore fluid) obtained. SP results in the current study are evaluated accordingly.

Acoustic Resonance Survey (Medford Cave)

24. The rationale for interpreting acoustic resonance data from simple features, as for example a shallow tunnel in soil, is that the maximum amplitude of the speaker-induced wave occurs immediately above the cavity feature. This has proven to be the case in previous investigations, but the features studied had usually been situated a few feet below the surface and the maximum horizontal feature dimensions had been on the order of 1 to 3 ft, typically. Medford Cave generally represented a much more complex condition, both in terms of depth of burial of the features and in terms of their size. However, in acoustic survey area 1, the cavity environment most closely approximated conditions previously studied and the acoustic amplitude contour plot shown in Figure 8 is centered on the known feature and does indicate its general extent. It had been recognized that larger and more complex features might not prove to be susceptible to such a simplistic approach, because the drastic changes in geometry could easily produce wave interference patterns, signal cancellation, beat frequencies, etc. It was argued that the signal received at the surface should attenuate as a function of range from the source, in a homogeneous medium, so that departures from this classic spatial pattern might be used as a means of detecting anomalous features (cavities).

25. An approach of this type was tried using the data obtained in acoustic survey area 1. The data as recorded at the site were of the form (x,y,a) where x and y represent the rectangular grid location of the measuring instrument and a the amplitude of the signal recorded at the location. The data were transformed to the form (d,a) where d represents the surface distance from the point directly above the signal source (106,260) to the recording instrument location. For this data set, the distances ranged from 1 to 61.61 ft, and the signal amplitude measured peak-to-peak ranged from 0 to 132 mv.

26. A least-squares fit was made to the attenuation data using various functional relations. The relation $a = A + B/d$ was selected as the best on the basis of an R-squared (square of the coefficient of correlation R) value of 0.41 and the fact that it gave reasonable predicted values $\hat{a}_i$ over the range of data. The data are plotted with the fitted curve shown in Figure 18.

27. The residuals from the relation $a = A + B/d$ are not normally distributed; therefore, Chebyshev's inequality (Hogg and Craig, 1970), $Pr(|a - \bar{a}| \geq KS) \leq 1/K^2$ is used to calculate the 93-percent (corresponding to $K = 3$) confidence interval. Chebyshev's inequality states that the random variable a is distributed about its mean value $\bar{a}$ according to the above relation for any positive number K, where S represents the standard deviation. The upper and lower bounds of the confidence interval in Figure 18 are curves fitted to the points calculated using the formula from Draper and Smith (1966):

$$\hat{a}_i \pm K \cdot S \cdot \sqrt{X_i^T \, C X_i}$$

where

$\hat{a}_i$ = the value of a in the relation $a = A + B/d$ corresponding to d_i

$K = 3$

S = the standard deviation of sample data

X_i^T = the vector $(1, d_i)$

$X_i = X_i^T$ transpose

The matrix $C = (X_i^T X)^{-1} = \frac{1}{n\Sigma(d_i-\bar{d})^2} \begin{bmatrix} \Sigma d_i^2 & -\Sigma d_i \\ -\Sigma d_i & n \end{bmatrix}$

and n equals the number of data points. Upper- and lower-bound curves for 93-percent confidence interval are also shown in Figure 18. A total of 40 data points fall above the upper-bound curve, and these data were normalized by dividing by the upper-bound curve value at the same range. The resulting set of 40 data points, ranging in amplitude ratio from 1.25 to 3.74, identify higher signal amplitudes than might be predicted from the upper-bound confidence curve. Since the rationale was that anomalously high amplitude signals should occur over a cavity feature(s), these data were used to develop the contour plot shown in Figure 19. Comparing Figures 8 and 19, it can be seen that the plot in Figure 19 appears to conform more closely to the WES-verified cavity location in acoustic survey area 1. Figures 20 and 21 present similarly derived plots of acoustic signal attenuation versus range from the source for acoustic survey areas 2 and 3, respectively. Comparing Figures 18, 20, and 21, it can be seen that considerably more data scatter is evident in Figures 20 and 21 than in Figure 18. Hence, it might be expected that the more complex features investigated in survey areas 2 and 3 might not be imaged so well by this method. Figures 22 and 23 present normalized signal attenuation contour plots for survey areas 2 and 3, respectively, and little improvement can be seen when comparing these with the original raw data contour plots (Figure 9 versus 22, Figure 10 versus 23). It appears that the signal attenuation versus range approach does not offer significant advantages when cavity features are both large and complex and are situated a few tens of feet below the ground surface. In an earlier investigation (Cooper and Bieganousky, 1978), the acoustic resonance technique had been successfully used to trace shallow solution cavities in limestone. Some of these cavity features were situated at depths comparable to the cavities at Medford Cave; however, the Medford Cave main cavity features are at least an order of magnitude larger in

lateral dimensions than the known cavity features previously investigated. So, it does appear that this acoustic resonance technique suffers a marked decrease in resolution when applied to large and complex cavernous features.

Sonar Study (Manatee Springs)

28. By inspection of Figure 17, it can be seen that easily measurable sonar signals could be propagated to distances of 200 ft or more from the source. This satisfied the primary question as to the feasibility of the approach. However, it can also be seen from Figure 17 that numerous areas of high-amplitude sonar signals were detected at points remote from the known main cavity channel. This result was unexpected, and unfortunately time and cost limitations precluded drilling these locations in an effort to develop a rationale for cause and effect. No signal attenuation methodology was applied since there appeared to be no consistent relationship between signal amplitude and cavity location.

29. It can be seen in Figure 17 that the right half of the sonar amplitude contour plot is comprised of very low level values. It is believed that the sonar signals did not effectively excite the main cavity system since the sonar source had to be located in the adjacent sinkhole because of the previously discussed limitations on submergence.

Self-Potential Survey (Manatee Springs)

30. In a situation where the direction of water flow is known, as at Manatee Springs, the reference electrode may be positioned upstream in which case the presence of a flow channel should certainly be indicated as a negative anomaly in the surface SP field. The geology of the Manatee Springs site suggests that the limestone is quite pervious, and in fact this has been verified by visual observations by cave divers, so that a negative bias in the SP field might be expected from water flowing through numerous small interconnected passages as well as in

major solution features within the survey zone. In fact, the raw SP contour plot presented in Figure 15 shows only one localized area where pronounced positive SP values were recorded.

31. In an attempt to gain better resolution in the SP survey plot, it was decided that the mean regional SP might be removed by subtracting the average SP value from each SP measurement. The average SP value was determined to be -25 mv, and using this value, a revised SP contour plot was developed as shown in Figure 24. Comparing Figure 15 (raw SP) with Figure 24 (residual SP), it can be seen that Figure 24 provides a spatial representation which is simpler and conforms better to the known location of cavity features. The zero SP residual contour area appears to crudely delineate the major zone of flow, although an exact delineation is probably not to be expected when the target system is located 90 ft below the ground surface. Only the areal extent of the system can be predicted using SP techniques developed to date; the prediction of depth is not yet within the state of the art.

Summary and Conclusions

32. It is concluded that the acoustic resonance technique is useful in delineating shallow (depth less than 20 ft) subsurface cavity features whose maximum horizontal dimensions are less than 10 feet, and that the interpretation in such cases is reasonably straightforward. However, as it usually the case with most geophysical techniques, increasing geologic complexity and depth of burial have drastic adverse effects on resolution. A sonar feasibility study was also conducted and it was demonstrated that a sonar source could deliver adequate energy to excite a deep water-filled cavity system; however, the known cavity features at Manatee Springs could not be delineated using the limited data obtained. The only NRL sonar source available at the time of this study was not well suited to site conditions, so this method may deserve further attention.

33. In this study the SP method was applied to the problem of detection and delineation of water-filled solution cavities in which

flow was occurring. A known large solution channel located at a depth of 90 ft was detected by surface methods, and a crude delineation of the feature was also achieved. There is as yet no technique for determining feature depth using surface SP methods. Improvement in cavity feature resolution was obtained in one phase of the Medford Cave acoustical survey and in the Manatee Springs SP survey by detrending the raw data based on (a) hypotheses as to the physical processes involved, and (b) careful observation of the apparent trends in the raw data. However, these techniques may not be applicable under all conditions.

REFERENCES

Ballard, R. F., Jr. 1977. "Dynamic Techniques for Detecting and Tracing Tunnel Complexes," Miscellaneous Paper S-77-25, U. S. Army Engineer Waterways Experiment Station, CE, Vicksburg, Miss.

Cooper, S. S., and Bieganousky, W. A. 1978. "Geophysical Survey of Cavernous Areas, Patoka Dam, Indiana," Miscellaneous Paper S-78-1, U. S. Army Engineer Waterways Experiment Station, CE, Vicksburg, Miss.

Corwin, R. F., and Hoover, D. B. 1979. "The Self-Potential Method in Geotechnical Exploration," Geophysics, Vol 44, No. 2, pp 226-245.

Draper, N. R., and Smith, H. 1966. Applied Regression Analysis, John Wiley & Sons, Inc., New York.

Groves, I. D., Jr. 1974. "Twenty Years of Underwater Electroacoustic Standards," Standards Branch, Underwater Sound Reference Division, Naval Research Laboratory, Report No. NRL-7735, Orlando, Fla.

Hogg, R. V., and Craig, A. T. 1970. Introduction to Mathematical Statistics, Third Edition, The Macmillan Company, New York.

Ogilvy, A. A., Ayed, M. A., and Bogoslovsky, V. A. 1969. "Geophysical Studies of Water Leakages from Reservoirs," Geophysical Prospecting, Vol 17, No. 1, pp 36-62.

Table 1

Acoustic Survey Data, Area No. 1

Grid S-N	Grid E-W	Signal Amp., volts	Grid S-N	Grid E-W	Signal Amp., volts	Grid S-N	Grid E-W	Signal Amp., volts
60.0	240.0	0.005	115.0	240.0	0.059	60.0	260.0	0.002
62.5	240.0	0.000	117.5	240.0	0.004	62.5	260.0	0.000
65.0	240.0	0.003	120.0	240.0	0.007	65.0	260.0	0.000
67.5	240.0	0.004	122.5	240.0	0.019	67.5	260.0	0.004
70.0	240.0	0.003	125.0	240.0	0.009	70.0	260.0	0.000
72.5	240.0	0.000	127.5	240.0	0.000	72.5	260.0	0.006
75.0	240.0	0.000	130.0	240.0	0.010	75.0	260.0	0.003
77.5	240.0	0.013	132.0	240.0	0.007	77.5	260.0	0.000
80.0	240.0	0.014	135.0	240.0	0.000	80.0	260.0	0.000
82.5	240.0	0.008	137.5	240.0	0.010	82.5	260.0	0.000
85.0	240.0	0.000	140.0	240.0	0.006	85.0	260.0	0.000
87.5	240.0	0.004	142.5	240.0	0.008	87.5	260.0	0.004
90.0	240.0	0.006	145.0	240.0	0.008	90.0	260.0	0.004
92.5	240.0	0.007	147.5	240.0	0.004	92.5	260.0	0.017
95.0	240.0	0.012	150.0	240.0	0.006	95.0	260.0	0.015
97.5	240.0	0.013	152.5	240.0	0.008	97.5	260.0	0.010
100.0	240.0	0.009	155.0	240.0	0.010	100.0	260.0	0.135
102.5	240.0	0.007	157.5	240.0	0.007	102.5	260.0	0.039
105.0	240.0	0.012	160.0	240.0	0.005	105.0	260.0	0.132
107.5	240.0	0.017				107.5	260.0	No data
110.0	240.0	0.016				110.0	260.0	0.040
112.5	240.0	0.013				112.5	260.0	No data
						115.0	260.0	No data

(Continued)

NOTE: Measured signal amplitudes are expressed in peak-to-peak volts read from an oscilloscope. To convert these readings to approximate peak-to-peak particle velocity in in inches per second, divide the voltage value by 10 (see text, page 11)

Table 1 (Continued)

Grid		Signal	Grid		Signal	Grid		Signal
S-N	E-W	Amp., volts	S-N	E-W	Amp., volts	S-N	E-W	Amp., volts
117.5	260.0	0.027	60.0	280.0	0.000	115.0	280.0	0.004
120.0	260.0	0.021	62.5	280.0	0.000	117.5	280.0	0.010
122.5	260.0	0.016	65.0	280.0	0.000	120.0	280.0	0.009
125.0	260.0	0.014	67.5	280.0	0.000	122.5	280.0	0.016
127.5	260.0	0.009	70.0	280.0	0.000	125.0	280.0	0.014
130.0	260.0	0.010	72.5	280.0	0.000	127.5	280.0	0.013
132.5	260.0	0.005	75.0	280.0	0.006	130.0	280.0	0.017
135.0	260.0	0.013	77.5	280.0	0.007	132.5	280.0	0.003
137.5	260.0	0.019	80.0	280.0	0.004	135.0	280.0	0.003
140.0	260.0	0.011	82.5	280.0	0.006	137.5	280.0	0.004
142.5	260.0	0.011	85.0	280.0	0.000	140.0	280.0	0.007
145.0	260.0	0.009	87.5	280.0	0.005	142.5	280.0	0.007
147.5	260.0	0.011	90.0	280.0	0.003	145.0	280.0	0.005
150.0	260.0	0.005	91.0	280.0	0.012	147.5	280.0	0.003
152.5	260.0	0.000	92.5	280.0	0.003	150.0	280.0	0.008
155.0	260.0	0.005	95.0	280.0	0.007	152.5	280.0	0.005
157.5	260.0	0.008	97.5	280.0	0.012	155.0	280.0	0.000
160.0	260.0	0.005	100.0	280.0	0.009	157.5	280.0	0.004
			102.5	280.0	0.012	160.0	280.0	0.005
			105.0	280.0	0.024			
			107.5	280.0	0.016			
			110.0	280.0	0.017			
			112.5	280.0	0.007			

(Continued)

Table 1 (Continued)

Grid		Signal	Grid		Signal	Grid		Signal
S-N	E-W	Amp., volts	S-N	E-W	Amp., volts	S-N	E-W	Amp., volts
140.0	240.0	0.007	120.0	240.0	0.007	100.0	240.0	0.011
140.0	242.5	0.007	120.0	242.5	0.023	100.0	242.5	0.011
140.0	245.0	0.010	120.0	245.0	0.017	100.0	245.0	0.007
140.0	247.5	0.005	120.0	247.5	0.010	100.0	247.5	0.006
140.0	250.0	0.003	120.0	250.0	0.016	100.0	250.0	0.019
140.0	252.5	0.004	120.0	252.5	0.025	100.0	252.5	0.007
140.0	255.0	0.011	120.0	255.0	0.015	100.0	255.0	0.010
140.0	257.5	0.017	120.0	257.5	0.004	100.0	257.5	0.066
140.0	260.0	0.011	120.0	260.0	0.021	100.0	260.0	0.135
140.0	262.5	0.007	120.0	262.5	0.023	100.0	262.5	0.137
140.0	265.0	0.006	120.0	265.0	0.018	100.0	265.0	0.029
140.0	267.5	0.004	120.0	267.5	0.006	100.0	267.5	0.020
140.0	270.0	0.003	120.0	270.0	0.018	100.0	269.0	0.115
140.0	272.5	0.003	120.0	272.5	0.008	100.0	270.0	0.075
140.0	275.0	0.013	120.0	275.0	0.006	100.0	272.5	0.036
140.0	277.5	0.005	120.0	277.5	0.007	100.0	275.0	0.027
140.0	280.0	0.007	120.0	280.0	0.009	100.0	277.5	0.009
						100.0	280.0	0.009
80.0	240.0	0.014	60.0	240.0	0.006	Miscellaneous Points		
80.0	242.5	0.007	60.0	242.5	0.003	109.0	252.0	0.084
80.0	245.0	0.005	60.0	245.0	0.004	112.0	248.0	0.037
80.0	247.5	0.009	60.0	247.5	0.002	111.0	245.0	0.025
80.0	250.0	0.013	60.0	250.0	0.002	125.0	235.0	0.024

(Continued)

Table 1 (Continued)

Grid		Signal	Grid		Signal	Grid		Signal
S-N	E-W	Amp., volts	S-N	E-W	Amp., volts	S-N	E-W	Amp., volts
80.0	252.5	0.016	60.0	252.5	0.002	128.0	230.0	0.012
80.0	255.0	0.004	60.0	255.0	0.000			
80.0	257.5	0.008	60.0	257.5	0.002			
80.0	260.0	0.000	60.0	260.0	0.000			
80.0	262.5	0.005	60.0	262.5	0.004			
80.0	265.0	0.003	60.0	265.0	0.010			
80.0	267.5	0.005	60.0	267.5	0.002			
80.0	270.0	0.008	60.0	270.0	0.006			
80.0	272.5	0.003	60.0	272.5	0.004			
80.0	275.0	0.009	60.0	275.0	0.003			
80.0	277.5	0.011	60.0	277.5	0.000			
80.0	280.0	0.004	60.0	280.0	0.000			
60.0	220.0	0.000	108.64	283.36	0.009			
61.52	221.98	0.000	110.16	285.34	0.003			
63.04	223.96	0.008	111.68	287.32	0.007			
64.56	225.94	0.005	113.20	289.30	0.005			
66.08	227.92	0.000	114.72	291.28	0.009			
67.60	229.90	0.006	116.24	293.26	0.007			
69.12	231.88	0.005	117.76	295.24	0.004			
70.64	233.86	0.013	119.24	297.22	0.009			
72.16	235.84	0.007	120.80	299.20	0.000			
73.68	237.82	0.000						
75.20	239.80	0.000						

(Continued)

Table 1 (Continued)

Grid		Signal	Grid		Signal	Grid		Signal
S-N	E-W	Amp., volts	S-N	E-W	Amp., volts	S-N	E-W	Amp., volts
76.72	241.78	0.007						
78.24	243.76	0.010						
79.76	245.74	0.000						
81.28	247.72	0.000						
82.80	249.70	0.000						
84.32	251.68	0.004						
85.84	253.66	0.007						
87.36	255.64	0.009						
88.88	257.62	0.018						
90.40	259.60	0.021						
91.92	261.58	0.036						
93.44	263.56	0.044						
94.96	265.54	0.014						
96.48	267.52	0.033						
98.00	269.50	0.019						
99.52	271.48	0.055						
101.04	273.46	0.016						
102.56	275.44	0.019						
104.08	277.42	0.022						
105.60	279.40	0.020						
107.12	281.38	0.024						
120.0	200.0	0.004						
120.0	202.5	0.003						

(Continued)

Table 1 (Concluded)

Grid		Signal	Grid		Signal	Grid		Signal
S-N	E-W	Amp., volts	S-N	E-W	Amp., volts	S-N	E-W	Amp., volts
120.0	205.0	0.003						
120.0	207.5	0.004						
120.0	210.0	0.005						
120.0	212.5	0.005						
120.0	215.0	0.000						
120.0	217.5	0.008						
120.0	220.0	0.006						
120.0	222.5	0.008						
120.0	225.0	0.019						
120.0	227.5	0.017						
120.0	230.0	0.005						
120.0	232.5	0.008						
120.0	235.0	0.023						
120.0	237.5	0.039						
120.0	240.0	0.007						

Table 2

Acoustic Survey Data, Area No. 2

Grid S-N	Grid E-W	Signal Amp., volts	Grid S-N	Grid E-W	Signal Amp., volts	Grid S-N	Grid E-W	Signal Amp., volts
140.0	120.0	0.006	140.0	140.0	0.029	140.0	160.0	0.005
142.5	120.0	0.009	142.5	140.0	0.006	142.5	160.0	0.016
145.0	120.0	0.009	145.0	140.0	0.010	145.0	160.0	0.021
147.5	120.0	0.005	147.5	140.0	0.021	147.5	160.0	0.017
150.0	120.0	0.022	150.0	140.0	0.022	150.0	160.0	0.125
152.5	120.0	0.007	152.5	140.0	0.080	152.5	160.0	0.022
155.0	120.0	0.010	155.0	140.0	0.087	155.0	160.0	0.023
157.5	120.0	0.013	157.5	140.0	0.201	157.5	160.0	0.013
160.0	120.0	0.031	160.0	140.0	0.061	160.0	160.0	0.075
162.5	120.0	0.061	162.5	140.0	0.013	162.5	160.0	0.034
165.0	120.0	0.051	165.0	140.0	0.015	165.0	160.0	0.092
167.5	120.0	0.051	167.5	140.0	0.008	167.5	160.0	0.118
170.0	120.0	0.039	170.0	140.0	0.025	170.0	160.0	0.080
172.5	120.0	0.070	172.5	140.0	0.055	172.5	160.0	0.083
175.0	120.0	0.051	175.0	140.0	0.030	175.0	160.0	0.057
177.5	120.0	0.045	177.5	140.0	0.038	177.5	160.0	0.050
180.0	120.0	0.041	180.0	140.0	0.034	180.0	160.0	0.021
140.0	122.5	0.011	160.0	122.5	0.020	180.0	122.5	0.011
140.0	125.0	0.009	160.0	125.0	0.023	180.0	125.0	0.012
140.0	127.5	0.003	160.0	127.5	0.008	180.0	127.5	0.012

(Continued)

NOTE: Measured signal amplitudes are expressed in peak-to-peak volts read from an oscilloscope. To convert these readings to approximate peak-to-peak particle velocity in inches per second, divide the voltage value by 10 (see text, page 11).

Table 2 (Continued)

Grid		Signal	Grid		Signal	Grid		Signal
S-N	E-W	Amp., volts	S-N	E-W	Amp., volts	S-N	E-W	Amp., volts
140.0	130.0	0.013	160.0	130.0	0.013	180.0	130.0	0.008
140.0	132.5	0.008	160.0	132.5	0.015	180.0	132.5	0.009
140.0	135.0	0.021	160.0	135.0	0.056	180.0	135.0	0.025
140.0	137.5	0.030	160.0	137.5	0.061	180.0	137.5	0.075
140.0	142.5	0.047	160.0	142.5	0.048	180.0	142.5	0.038
140.0	145.0	0.011	160.0	145.0	0.123	180.0	145.0	0.033
140.0	147.5	0.040	160.0	147.5	0.050	180.0	147.5	0.034
140.0	150.0	0.011	160.0	150.0	0.092	180.0	150.0	0.039
140.0	152.5	0.013	160.0	152.5	0.102	180.0	152.5	0.074
140.0	155.0	0.006	160.0	155.0	0.018	180.0	155.0	0.067
150.0	157.0	0.044	160.0	157.5	0.030	180.0	157.5	0.047
178.2	121.8	0.020	178.2	141.8	0.043	158.2	121.8	0.041
176.4	123.6	0.011	176.4	143.6	0.020	156.4	123.6	0.049
174.6	125.4	0.013	174.6	145.4	0.030	154.6	125.4	0.021
172.8	127.2	0.011	172.8	147.2	0.046	152.8	127.2	0.030
171.1	129.0	0.010	171.1	149.0	0.058	151.0	129.0	0.004
169.2	130.8	0.010	169.2	150.8	0.076	149.2	130.8	0.008
167.4	132.6	0.033	167.4	152.6	0.109	147.4	132.6	0.017
165.6	134.4	0.020	165.6	154.4	0.060	145.5	134.4	0.012
163.8	136.2	0.013	163.8	156.2	0.051	143.8	136.2	0.014
162.0	138.0	0.019	162.0	158.0	0.017	142.0	138.0	0.011
158.2	141.8	0.019						
156.4	143.6	0.088						

(Continued)

Table 2 (Concluded)

Grid		Signal	Grid		Signal	Grid		Signal
S-N	E-W	Amp., volts	S-N	E-W	Amp., volts	S-N	E-W	Amp., volts
154.6	145.4	0.089						
152.8	147.2	0.053						
151.0	149.0	0.025						
149.2	150.8	0.031						
147.4	152.6	0.015						
145.6	154.4	0.021						
143.8	156.2	0.014						
142.0	158.0	0.008						

Table 3

Acoustic Survey Data, Area No. 3

Grid S-N	Grid E-W	Signal Amp., volts	Grid S-N	Grid E-W	Signal Amp., volts	Grid S-N	Grid E-W	Signal Amp., volts
100.0	100.0	0.004	100.0	120.0	0.005	100.0	140.0	0.006
102.5	100.0	0.004	102.5	120.0	0.000	102.5	140.0	0.003
105.0	100.0	0.003	105.0	120.0	0.000	105.0	140.0	0.003
107.5	100.0	0.005	107.5	120.00	0.003	107.5	140.0	0.000
110.0	100.0	0.006	110.0	120.0	0.007	110.0	140.0	0.013
112.5	100.0	0.003	112.5	120.0	0.005	112.5	140.0	0.011
115.0	100.0	0.006	115.0	120.0	0.016	115.0	140.0	0.012
117.5	100.0	0.004	117.5	120.0	0.010	117.5	140.0	0.013
120.0	100.0	0.003	120.0	120.0	0.007	120.0	140.0	0.024
122.5	100.0	0.000	122.5	120.0	0.013	122.5	140.0	0.024
125.0	100.0	0.005	125.0	120.0	0.036	125.0	140.0	0.011
127.5	100.0	0.005	127.5	120.0	0.017	127.5	140.0	0.007
130.0	100.0	0.008	130.0	120.0	0.024	130.0	140.0	0.018
132.5	100.0	0.005	132.5	120.0	0.028	132.5	140.0	0.027
135.0	100.0	0.005	135.0	120.0	0.029	135.0	140.0	0.011
137.5	100.0	0.006	137.5	120.0	0.015	137.5	140.0	0.018
140.0	100.0	0.009	140.0	120.0	0.031	140.0	140.0	0.000
142.5	100.0	0.006	142.5	120.0	0.028	142.5	140.0	0.016
145.0	100.0	0.003	145.0	120.0	0.023	145.0	140.0	0.032
147.5	100.0	0.007	147.2	120.0	0.009	147.5	140.0	0.058
150.0	100.0	0.008	150.0	120.0	0.016	150.0	140.0	0.028
152.5	100.0	0.006	152.5	120.0	0.038	152.5	140.0	0.045

(Continued)

NOTE: Measured signal amplitudes are expressed in peak-to-peak volts read from an oscilloscope. To convert these readings to approximate peak-to-peak particle velocity in in inches per second, divide the voltage value by 10 (see text, page 11).

Table 3 (Continued)

Grid		Signal	Grid		Signal	Grid		Signal
S-N	E-W	Amp., volts	S-N	E-W	Amp., volts	S-N	E-W	Amp., volts
155.0	100.0	0.008	155.0	120.0	0.036	155.0	140.0	0.045
157.5	100.0	0.008	157.5	120.0	0.026	157.5	140.0	0.042
160.0	100.0	0.015	160.0	120.0	0.023	160.0	140.0	0.025
162.5	100.0	0.006	162.5	120.0	0.021	162.5	140.0	0.012
165.0	100.0	0.006	165.0	120.0	0.015	165.0	140.0	0.008
167.5	100.0	0.005	167.5	120.0	0.014	167.5	140.0	0.000
170.0	100.0	0.007	170.0	120.0	0.005	170.0	140.0	0.007
172.5	100.0	0.000	172.5	120.0	0.008	172.5	140.0	0.006
175.0	100.0	0.000	175.0	120.0	0.006	175.0	140.0	0.005
177.5	100.0	0.000	177.5	120.0	0.012	177.5	140.0	0.003
180.0	100.0	0.002	180.0	120.0	0.008	180.0	140.0	0.006
120.0	160.0	0.004	180.0	102.5	0.003	160.0	102.5	0.009
122.5	160.0	0.012	180.0	105.0	0.002	160.0	105.0	0.002
125.0	160.0	0.003	180.0	107.5	0.003	160.0	107.5	0.003
127.5	160.0	0.005	180.0	110.0	0.000	160.0	110.0	0.006
130.0	160.0	0.006	180.0	112.5	0.005	160.0	112.5	0.003
132.5	160.0	0.004	180.0	115.0	0.006	160.0	115.0	0.003
135.0	160.0	0.004	180.0	117.5	0.003	160.0	117.5	0.009
137.5	160.0	0.006	180.0	122.5	0.000	160.0	122.5	0.000
140.0	160.0	0.008	180.0	125.0	0.000	160.0	125.0	0.011
142.5	160.0	0.010	180.0	127.5	0.000	160.0	127.5	0.010
145.0	160.0	0.011	180.0	130.0	0.000	160.0	130.0	0.007

(Continued)

Table 3 (Continued)

Grid S-N	Grid E-W	Signal Amp., volts	Grid S-N	Grid E-W	Signal Amp., volts	Grid S-N	Grid E-W	Signal Amp., volts
147.5	160.0	0.008	180.0	132.5	0.000	160.0	132.5	0.018
150.0	160.0	0.013	180.0	135.0	0.000	160.0	135.0	0.023
152.5	160.0	0.011	180.0	137.5	0.000	160.0	137.5	0.018
155.0	160.0	0.012	180.0	142.5	0.000	160.0	142.5	0.021
157.5	160.0	0.005	180.0	145.0	0.000	160.0	145.0	0.028
160.0	160.0	0.009	180.0	147.5	0.000	160.0	147.5	0.037
162.5	160.0	0.005	180.0	150.0	0.000	160.0	150.0	0.020
165.0	160.0	0.020	180.0	152.5	0.000	160.0	152.5	0.029
167.5	160.0	0.015	180.0	155.0	0.007	160.0	155.0	0.010
170.0	160.0	0.010	180.0	157.5	0.000	160.0	157.5	0.018
172.5	160.0	0.013						
175.0	160.0	0.010						
177.5	160.0	0.004						
180.0	160.0	0.035						
100.0	160.0	0.000						
102.5	160.0	0.000						
105.0	160.0	0.000						
107.5	160.0	0.000						
110.0	160.0	0.000						
112.5	160.0	0.000						
115.0	160.0	0.000						
117.5	160.0	0.000						

(Continued)

Table 3 (Concluded)

Grid		Signal	Grid		Signal	Grid		Signal
S-N	E-W	Amp., volts	S-N	E-W	Amp., volts	S-N	E-W	Amp., volts
140.0	102.5	0.000	120.0	102.5	0.004	100.0	102.5	0.000
140.0	105.0	0.000	120.0	105.0	0.017	100.0	105.0	0.005
140.0	107.5	0.000	120.0	107.5	0.008	100.0	107.5	0.005
140.0	110.0	0.007	120.0	110.0	0.005	100.0	110.0	0.000
140.0	112.5	0.013	120.0	112.5	0.009	100.0	112.5	0.000
140.0	115.0	0.009	120.0	115.0	0.003	100.0	115.0	0.000
140.0	117.5	0.010	120.0	117.5	0.003	100.0	117.5	0.000
140.0	122.5	0.016	120.0	122.5	0.006	100.0	122.5	0.000
140.0	125.0	0.010	120.0	125.0	0.010	100.0	125.0	0.000
140.0	127.5	0.016	120.0	127.5	0.003	100.0	127.5	0.006
140.0	130.0	0.011	120.0	130.0	0.006	100.0	130.0	0.008
140.0	132.5	0.040	120.0	132.5	0.003	100.0	132.5	0.003
140.0	135.0	0.021	120.0	135.0	0.005	100.0	135.0	0.013
140.0	137.5	0.021	120.0	137.5	0.010	100.0	137.5	0.003
140.0	142.5	0.00_	120.0	142.5	0.023	100.0	142.5	0.000
140.0	145.0	0.011	120.0	145.0	0.011	100.0	145.0	0.000
140.0	147.5	0.018	120.0	147.5	0.016	100.0	147.5	0.000
140.0	150.0	0.008	120.0	150.0	0.012	100.0	150.0	0.000
140.0	152.5	0.000	120.0	152.5	0.006	100.0	152.5	0.000
140.0	155.0	0.009	120.0	155.0	0.005	100.0	155.0	0.000
140.0	157.5	0.008	120.0	157.5	0.004	100.0	157.5	0.000

Table 4

Self-Potential Survey Data, Manatee Springs

North 45 deg West	North 45 deg East																			
	0	10	20	30	40	50	60	70	80	90	100	110	120	130	140	150	160	170	180	190	200
0	-32	-38	-34	-40	-22	-28	-37	-34	-44	-42	-47	-21	-50	-10	-27	-22	-43	-25	-23	-11	-26
20	-39	-39	-19	-18	-15	-27	-15	-15	-19	-25	-25	-9	-11	-18	-44	-22	-63	-31	-53	-33	-47
40	-30	-7	-21	-26	-32	-19	-14	-15	-26	-31	-17	+1	-9	-33	-53	-54	-31	-37	-21	-26	-41
60	-25	-17	-25	-26	-32	-19	-16	-20	-32	+6	+96	+43	+23	+3	-19	-12	-23	-82	-32	-41	-12
80	-8	-25	-11	-32	-12	-3	-49	-30	-27	-25	-27	-5	-15	-48	-36	-25	-20	-15	-56	-23	-24
100	-63	-23	-20	-25	-56	-13	-28	-5	-25	-16	-47	-26	-39	-27	-32	-30	-24	-36	-44	-19	-5
120							-21	-13	-16	-27	-26	-58	-18	-60	-74	-40	-50	-30	-32	-21	-20

	210	220	230	240	250	260	270	280	290	300	310	320	330	340	350	360	370	380	390	400
0	-30	-38	-13	-5	-14	+1	-12	-5	-2	+6	+5	+6	+7	-5	-12	-12	-30	-54	-64	-33
20	-17	-24	-19	-23	-26	-32	-58	-11	-16	-31	-5	-10	-19	-23	-35	-21	-18	-12	-26	-38
40	-38	-18	-25	-32	-65	-25	-20	-44	-49	-23	-61	-36	-4	-20	-40	-18	-42	-33	-32	-20
60	-32	-26	-42	-30	+18	-20	-72	-26	-50	-24	-35	-30	-10	-28	-23	-29	-18	-28	-18	-13
80	-35	+9	-15	-60	-48	-54	-27	-45	-40	-47	-40	-4	+5	+3	-3	-10	-40	-33	-43	-32
100	-3	-17	-68	-49	-30	-44	-54	-44	-40	-7	-8	-4	-8	-3	-6	-19	-28	-26	-28	-56
120	+1	-2	-15	-45	-31	-47	-30													

NOTE: Readings are expressed in millivolts DC read between the survey and reference electrodes.

Table 5

Sonar Data, Manatee Springs Site

North 45 deg West	North 45 Deg East																				
	0	20	40	60	80	100	120	140	160	180	200	220	240	260	280	300	320	340	360	380	400
0	3.0	2.0	5.0	0.5	0.75	0.75	3.0	3.5	3.0	0.75	1.0	0.75	0.5	0.75	0.5	0.75	0.0	0.0	1.0	0.0	0.0
20	2.5	2.0	1.5	1.75	0.75	1.75	1.5	2.0	6.0	3.0	1.5	1.75	1.25	0.0	0.75	0.0	0.75	0.0	0.0	1.5	0.75
40	2.0	1.25	0.0	2.0	0.50	4.0	6.0	2.5	6.0	4.0	3.0	1.75	1. 5	1.25	0.0	0.0	0.0	0.0	0.0	0.0	0.0
60	4.0	3.0	1.0	2.5	1.75	2.5	0.0	0.5	1.75	3.0	0.0	2.0	2.0	0.50	1.0	0.0	0.0	0.0	0.0	0.0	0.0
80	5.5	2.0	3.0	0.75	1.0	3.0	1.25	2.0	1.75	3.75	5.0	3.0	5.5	0.0	2.0	2.5	1.5	0.5	0.2	0.0	0.0
100						2.5	2.0	3.0	2.0	2.0	0.5	3.0	1.0	0.5	0.0	0.0					

NOTE: Measured signal amplitudes are expressed in peak-to-peak volts read from an oscilloscope. To convert these readings to approximate peak-to-peak particle velocity, divide the voltage value by 400 (see text, page 13).

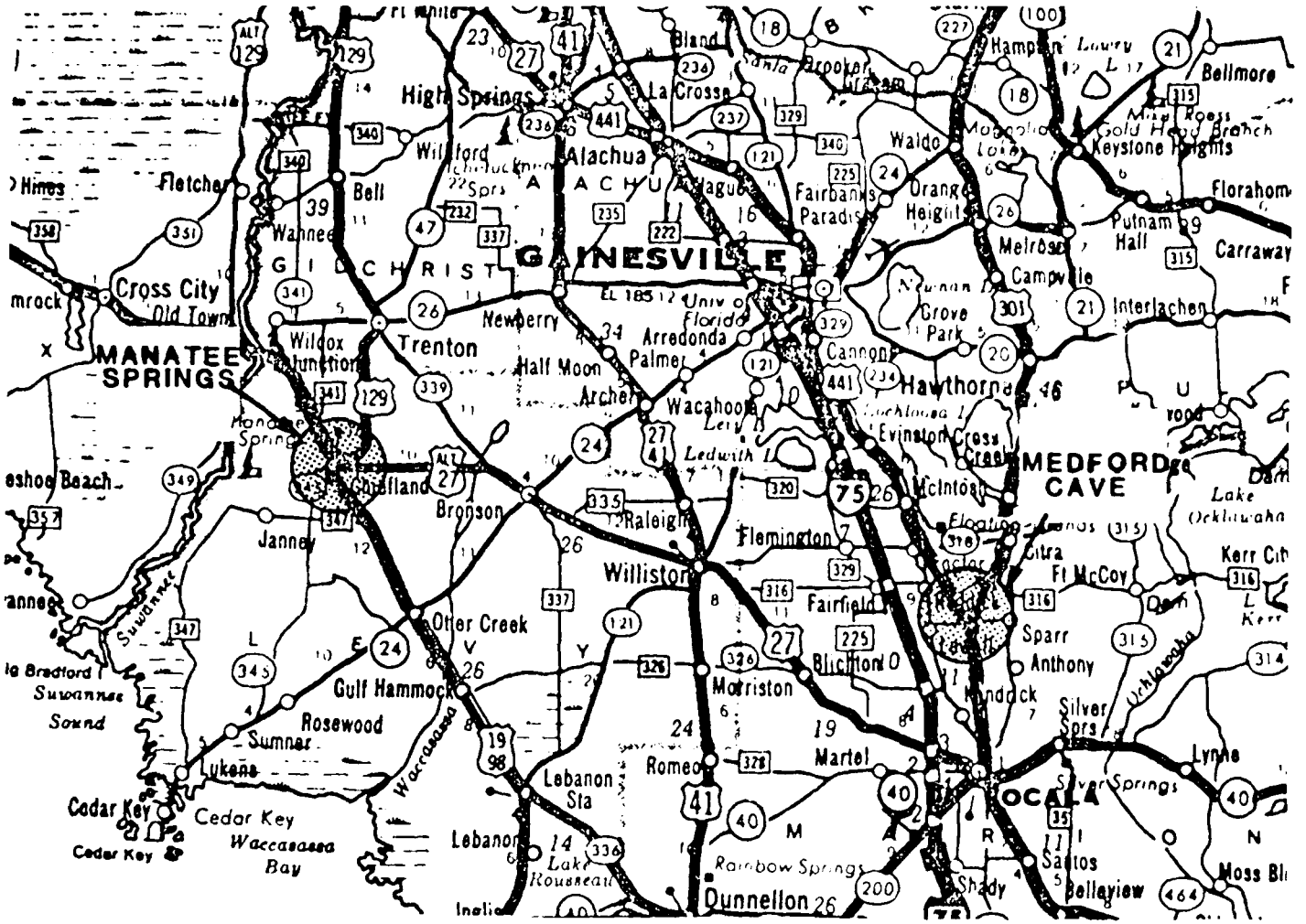

Figure 1. Location of Medford Cave and Manatee Springs test sites

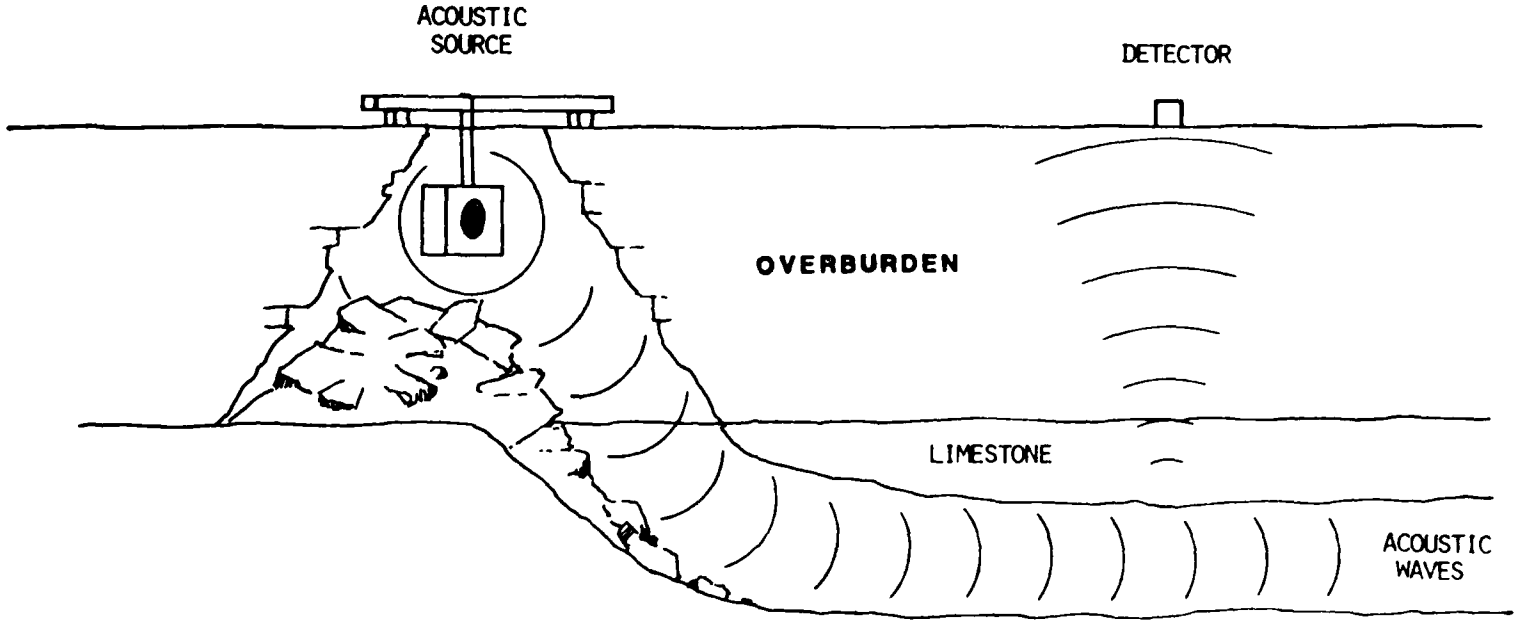

Figure 2. Typical equipment configuration for an acoustic resonance survey

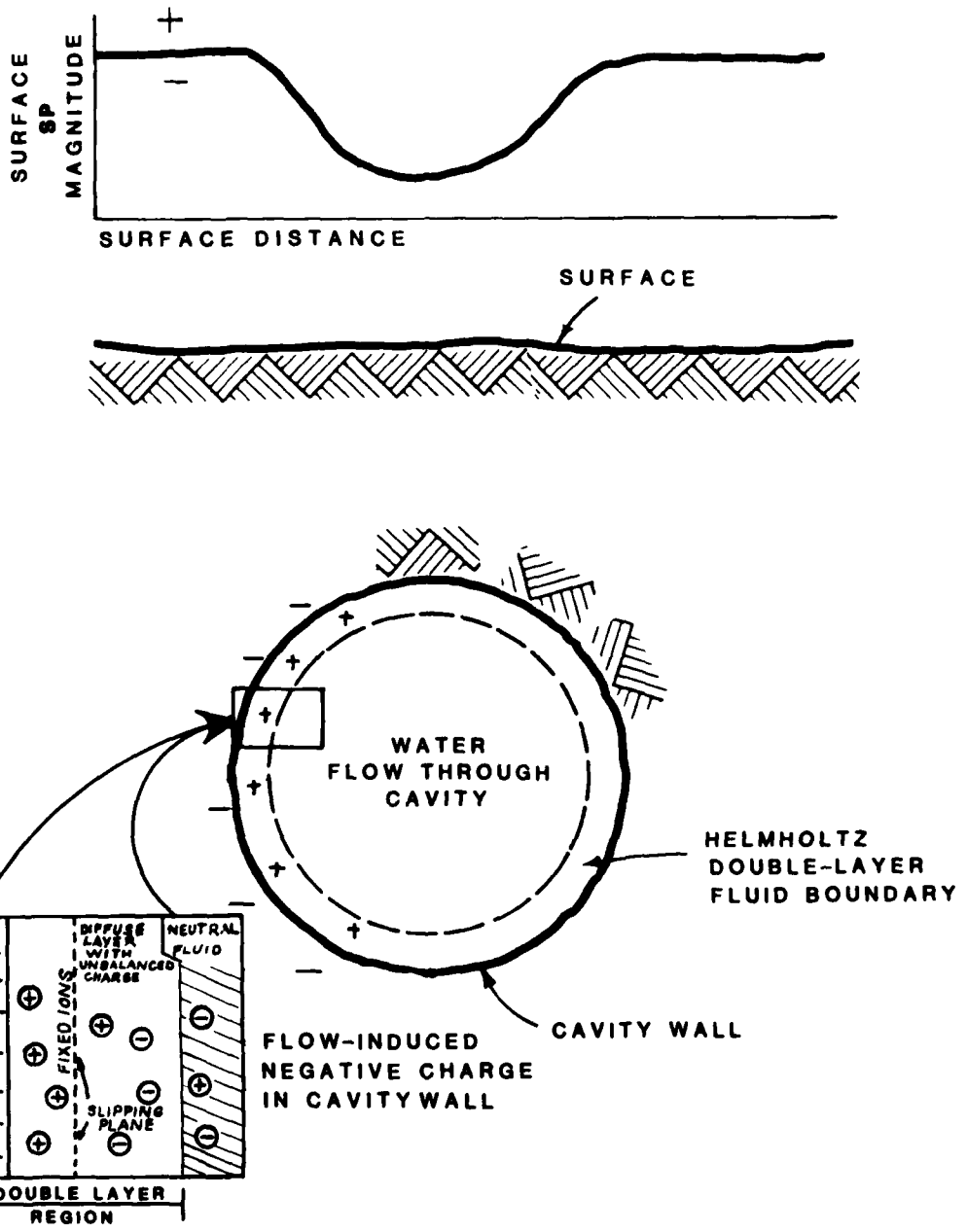

Figure 3. Origin of flow-induced negative self-potentials

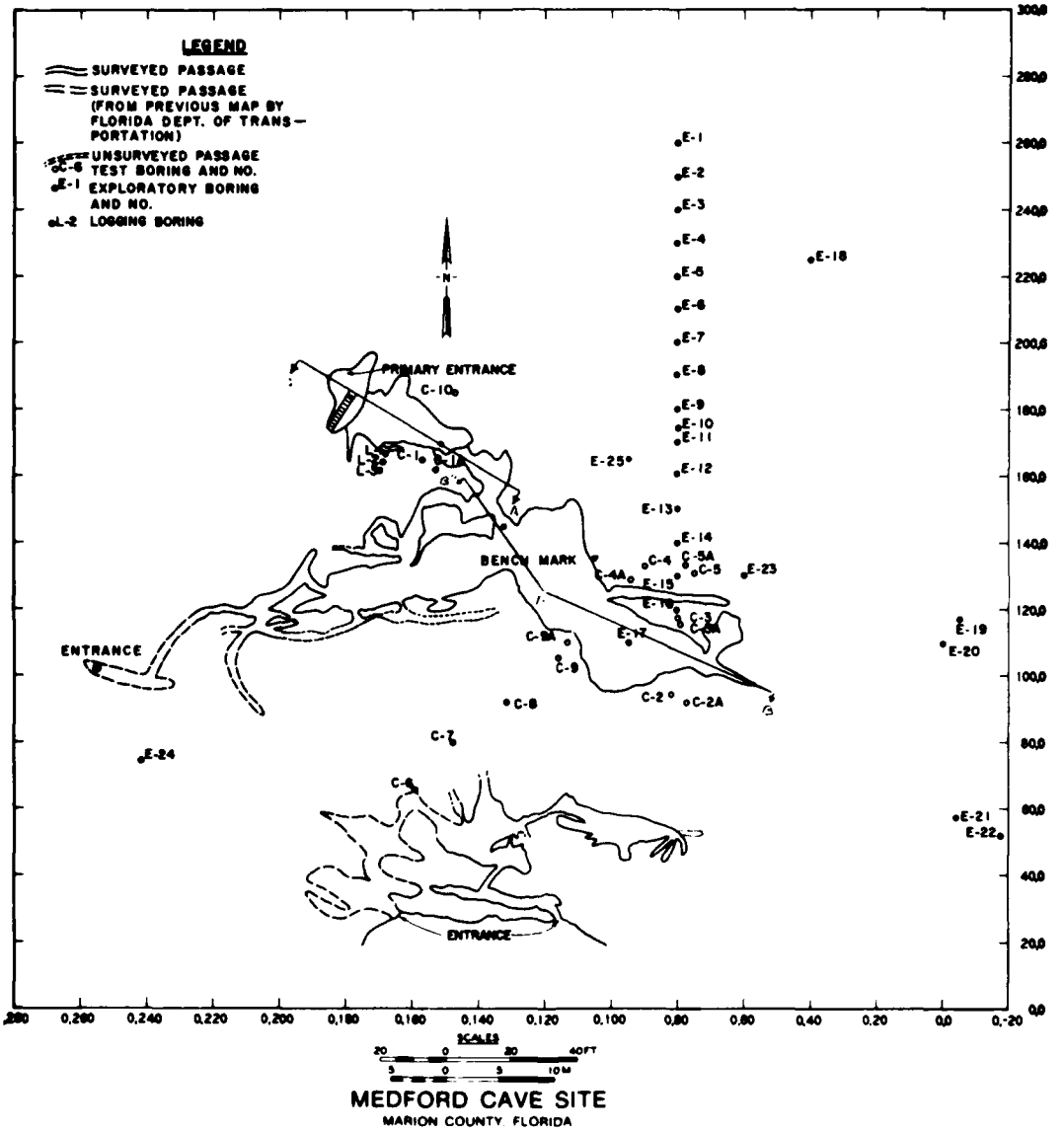

Figure 4. Plan view of the Medford Cave test site showing cavity system, boring, and profile locations

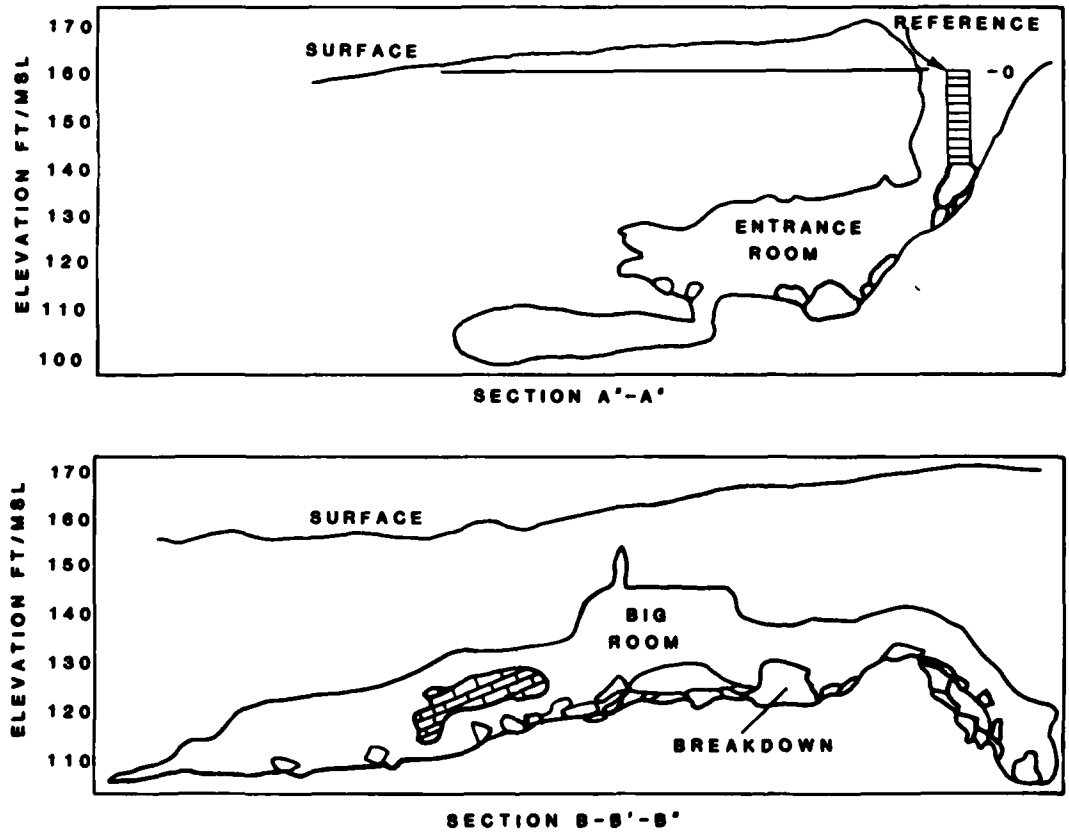

Figure 5. Typical cross sections through the Medford Cave main cavity system

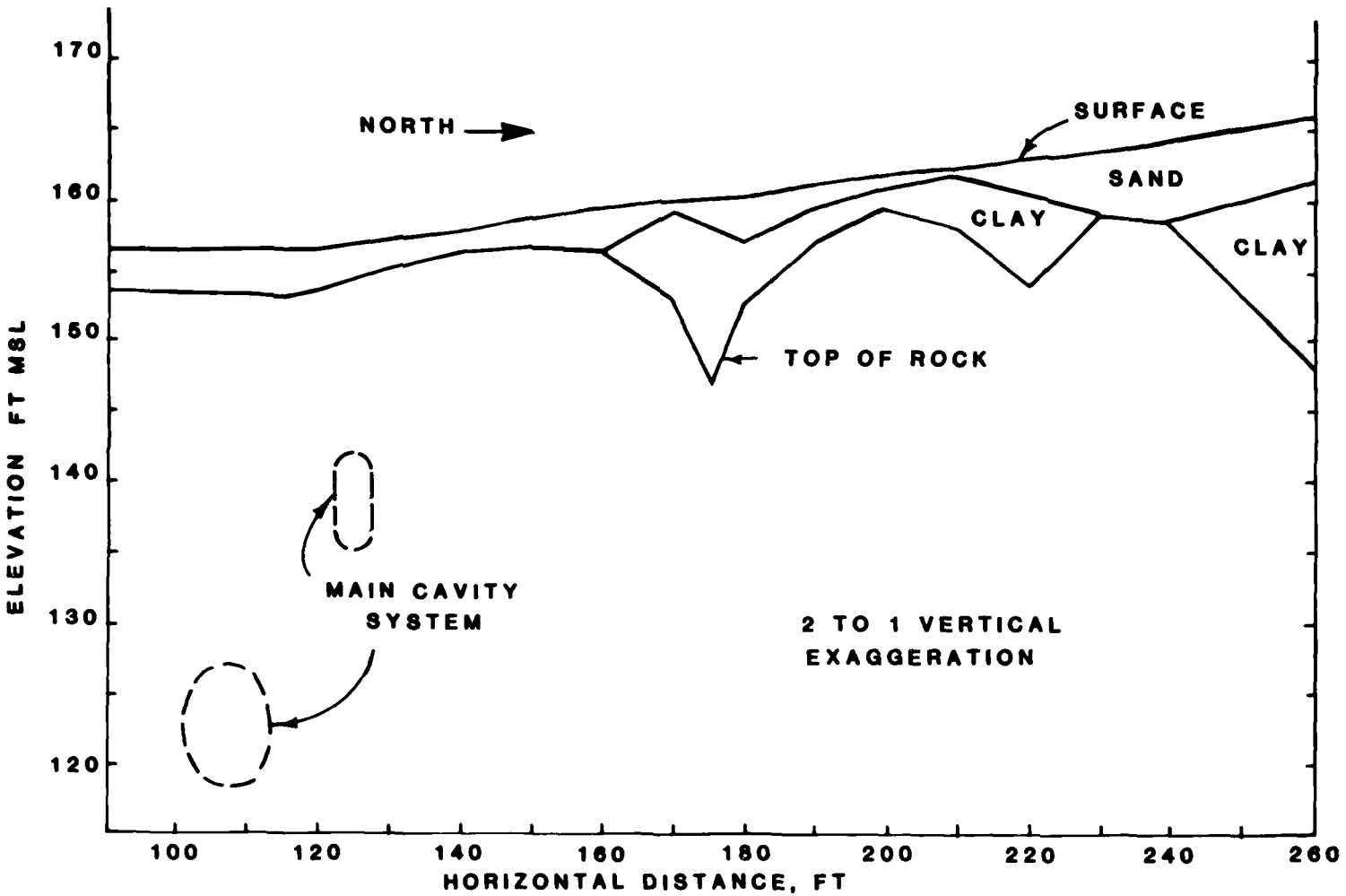

Figure 6. Subsurface profile along the 80 north grid line

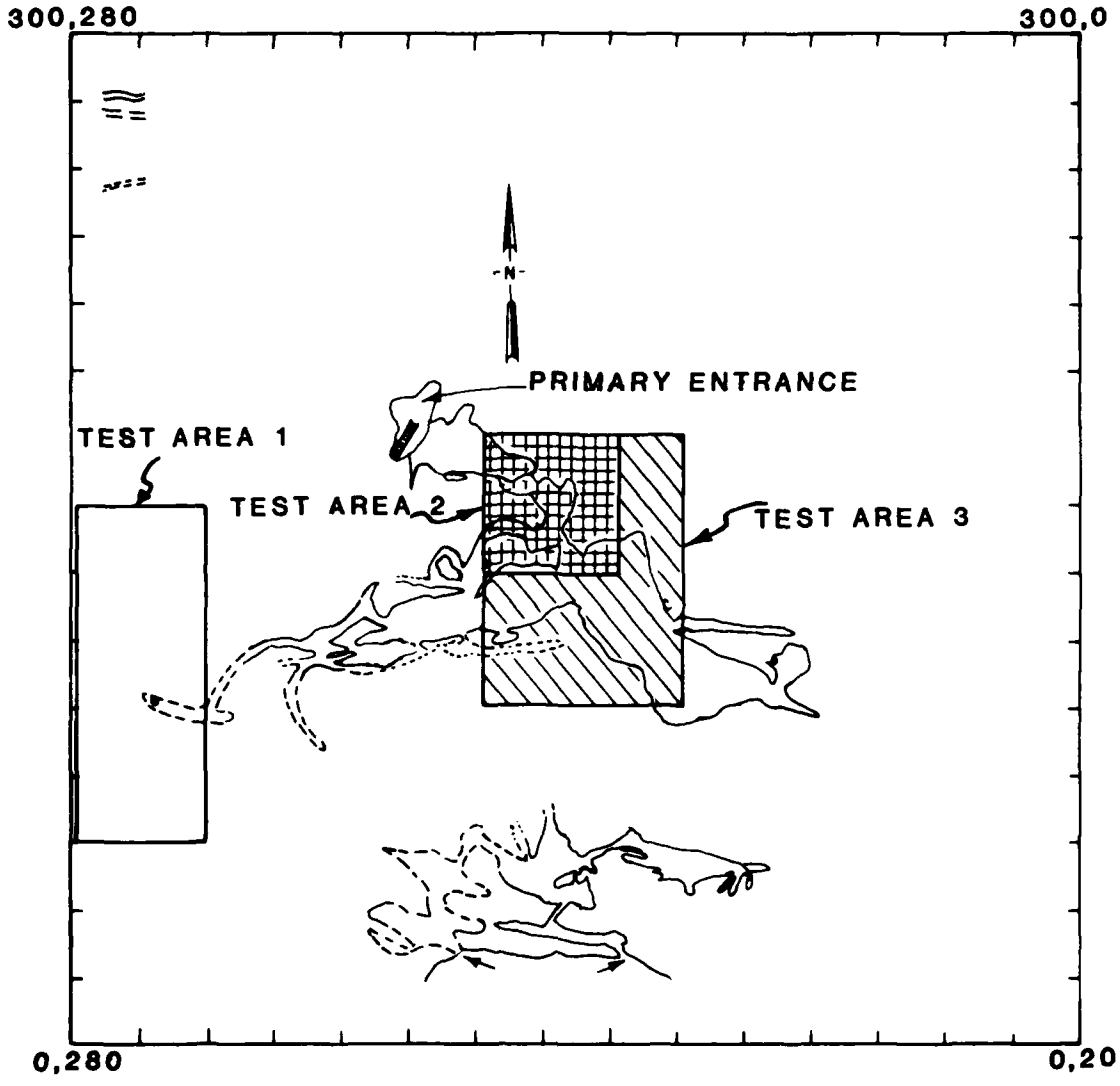

Figure 7. Location of acoustic resonance survey areas with respect to the main cavity system, Medford Cave

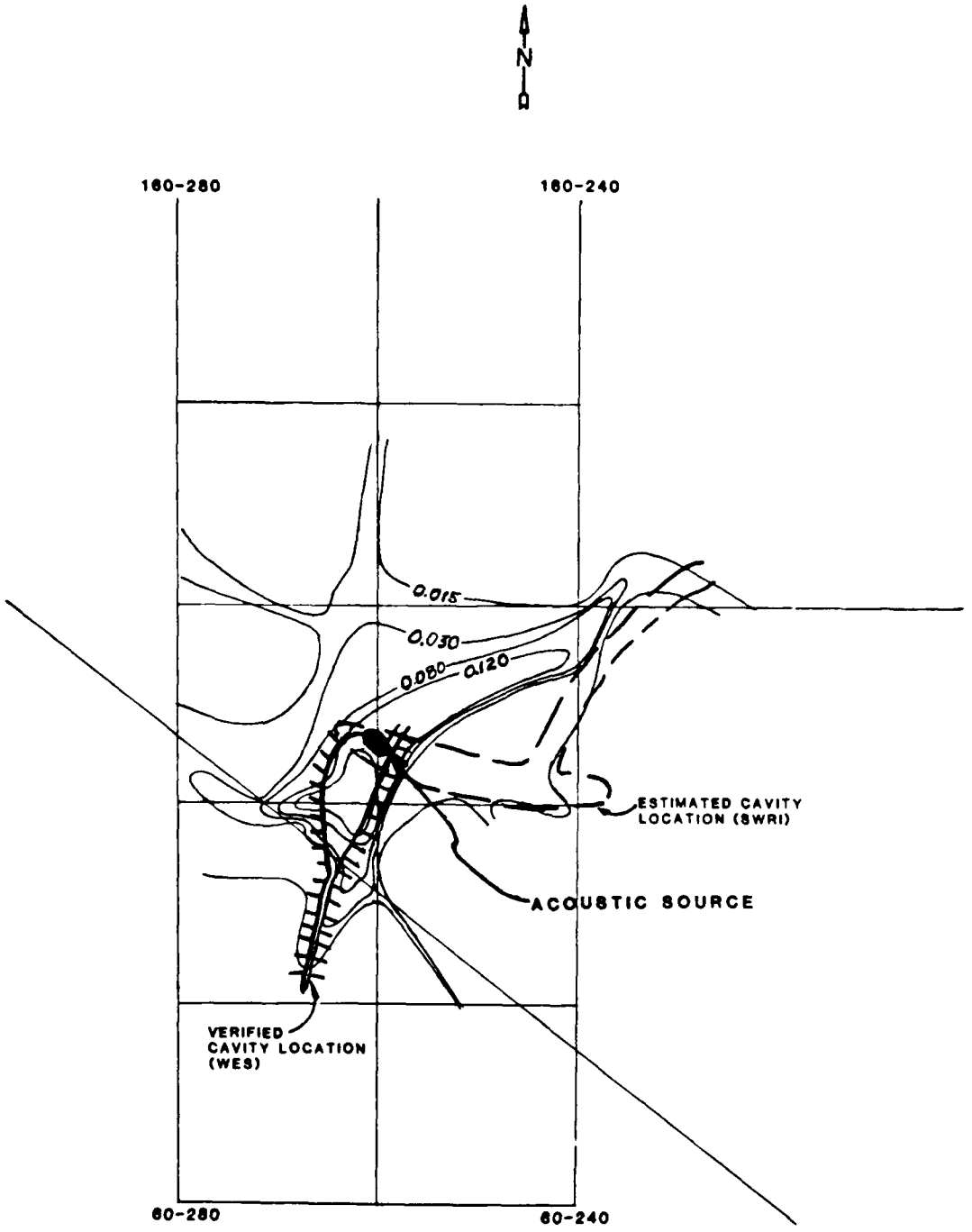

Figure 8. Contour plot of acoustic signal magnitude showing location of acoustic source, test area 1, Medford Cave

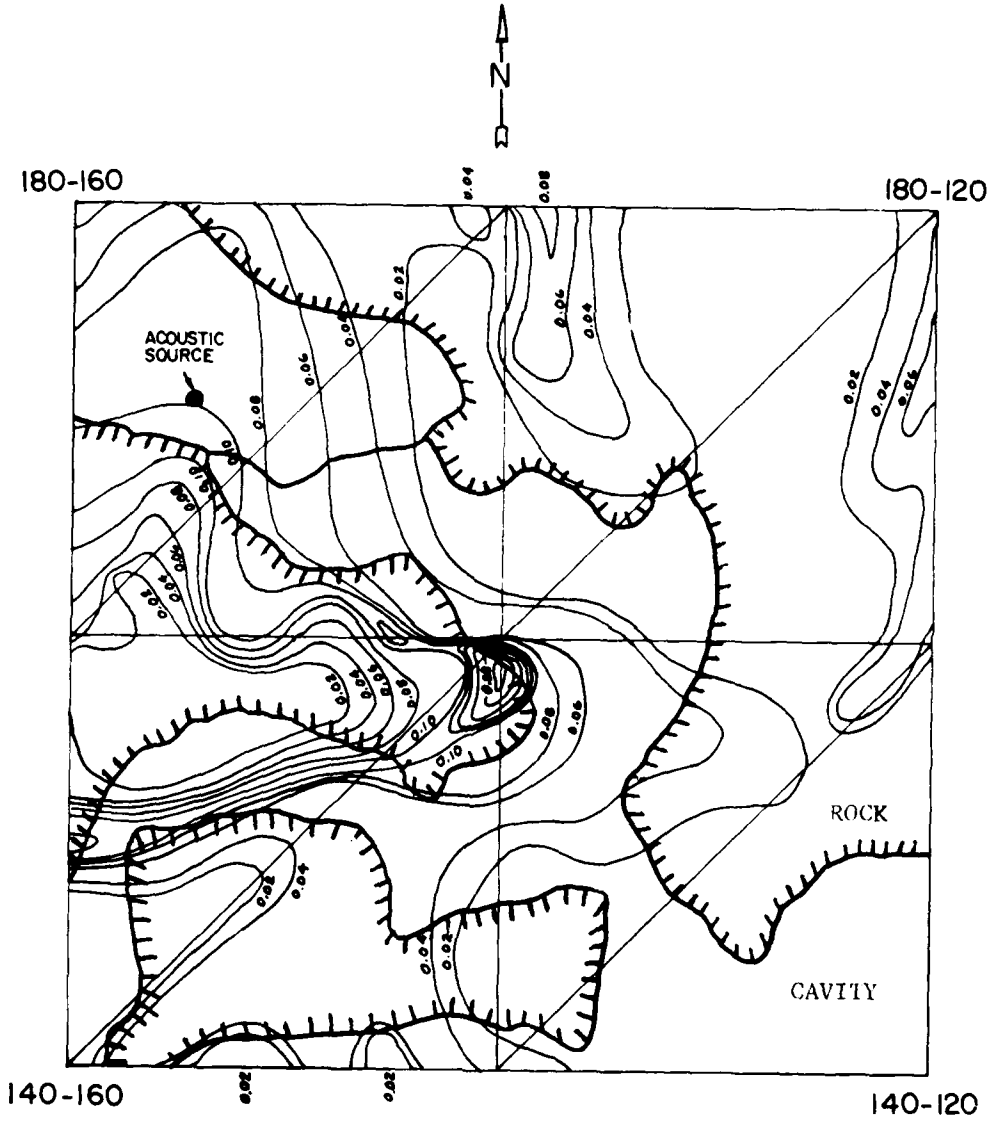

Figure 9. Contour plot of acoustic signal magnitude showing location of acoustic source, test area 2, Medford Cave

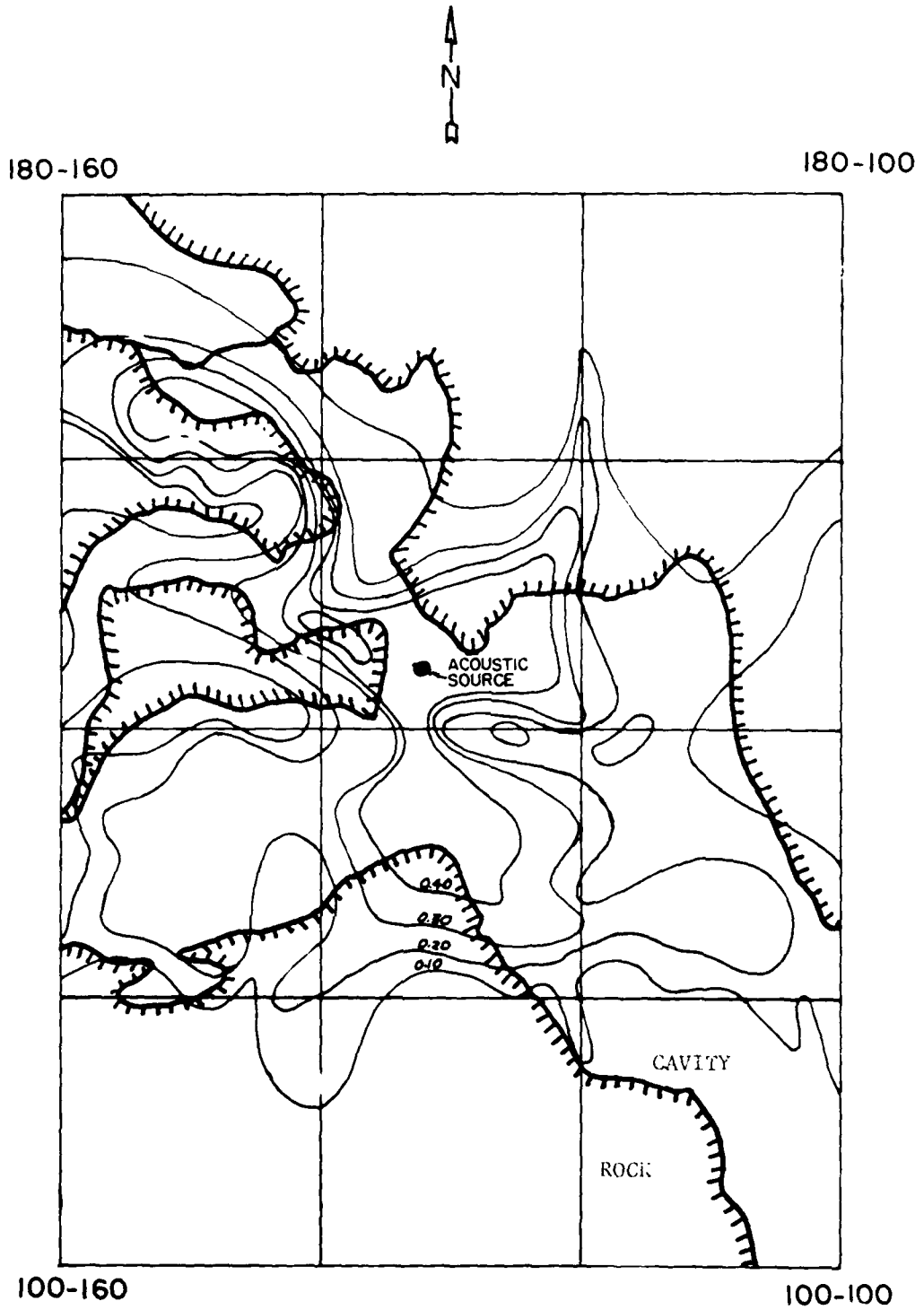

Figure 10. Contour plot of acoustic signal magnitude showing location of acoustic source, test area 3, Medford Cave

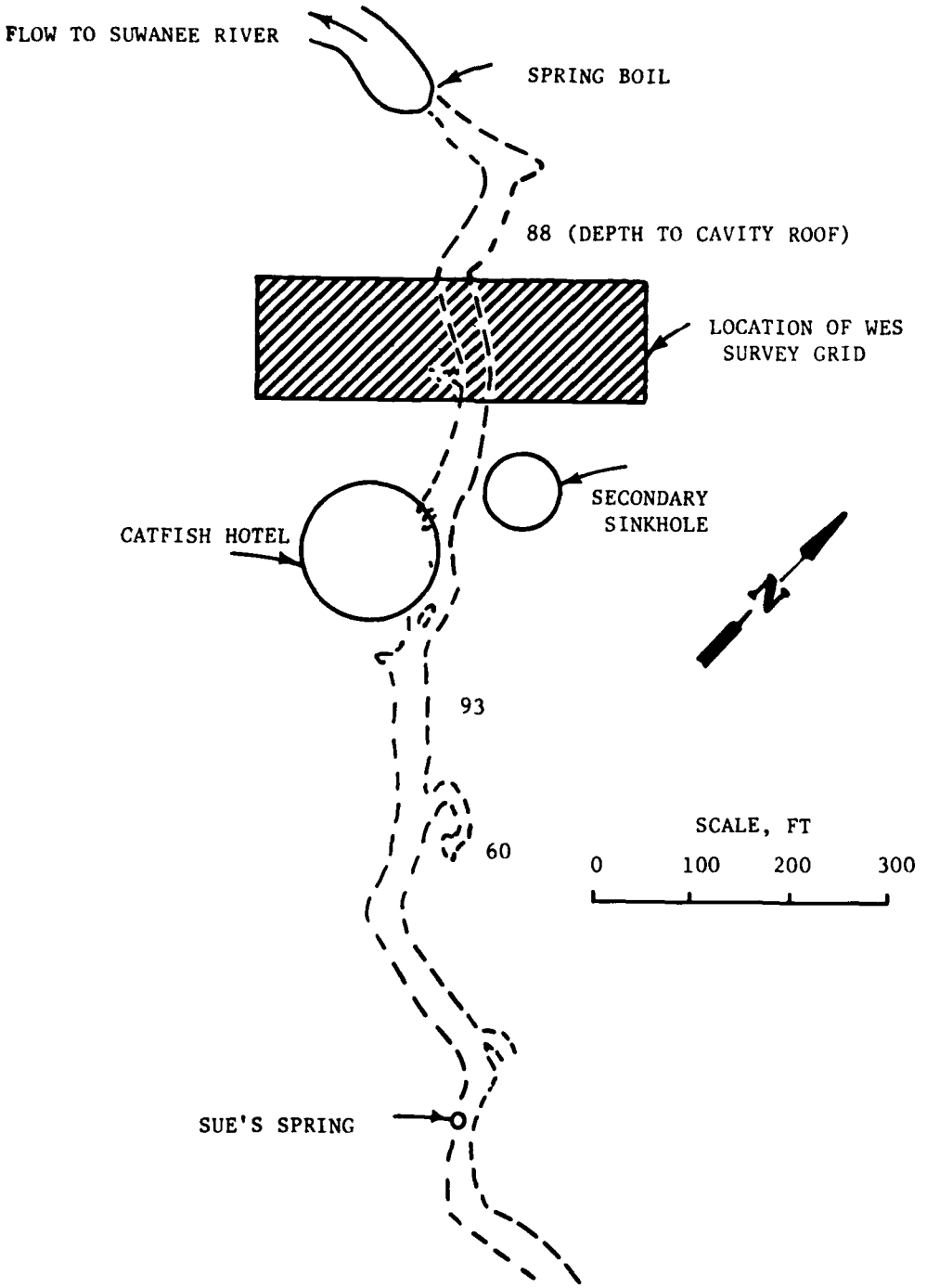

Figure 11. Plan view of the Manatee Springs site showing general trend of main cavity and location of WES survey grid

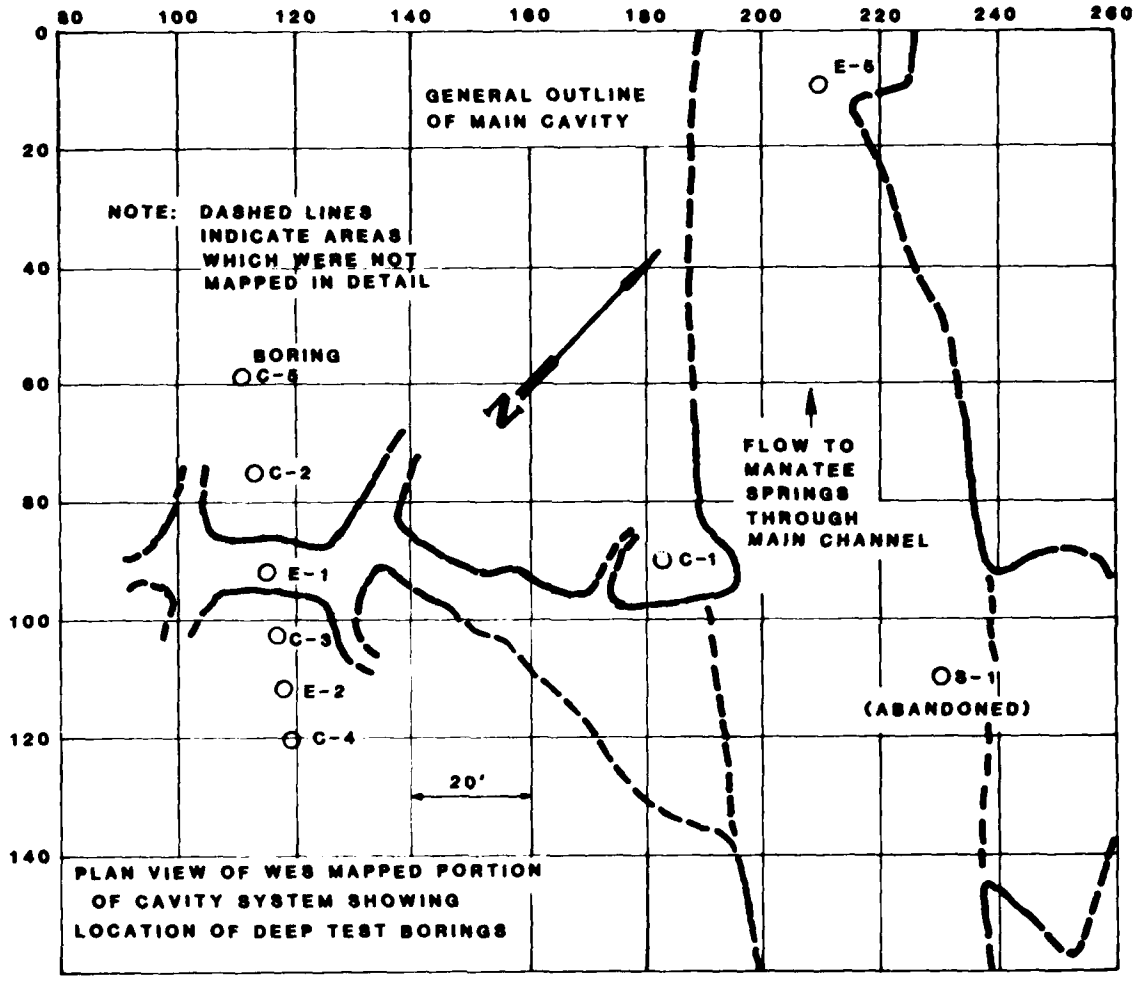

Figure 12. Location of WES survey area at Manatee Springs test site showing boring locations and general outline of main cavity

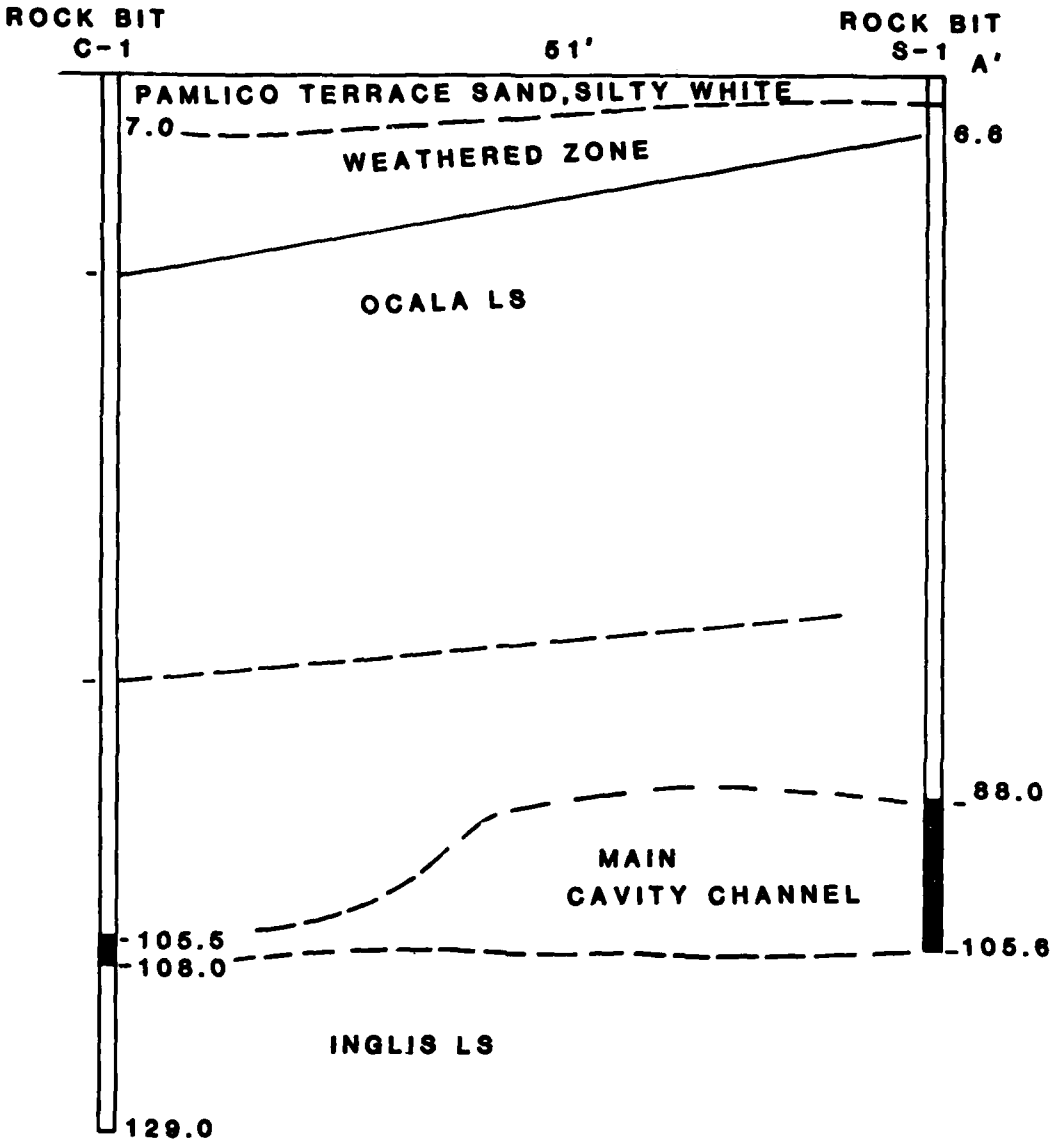

GEOLOGIC PROFILE A-A'

HORIZONTAL SCALE 1" 10'

VERTICAL SCALE 1" 20'

Figure 13. Cross section between borings C-1 and S-1 showing main cavity system

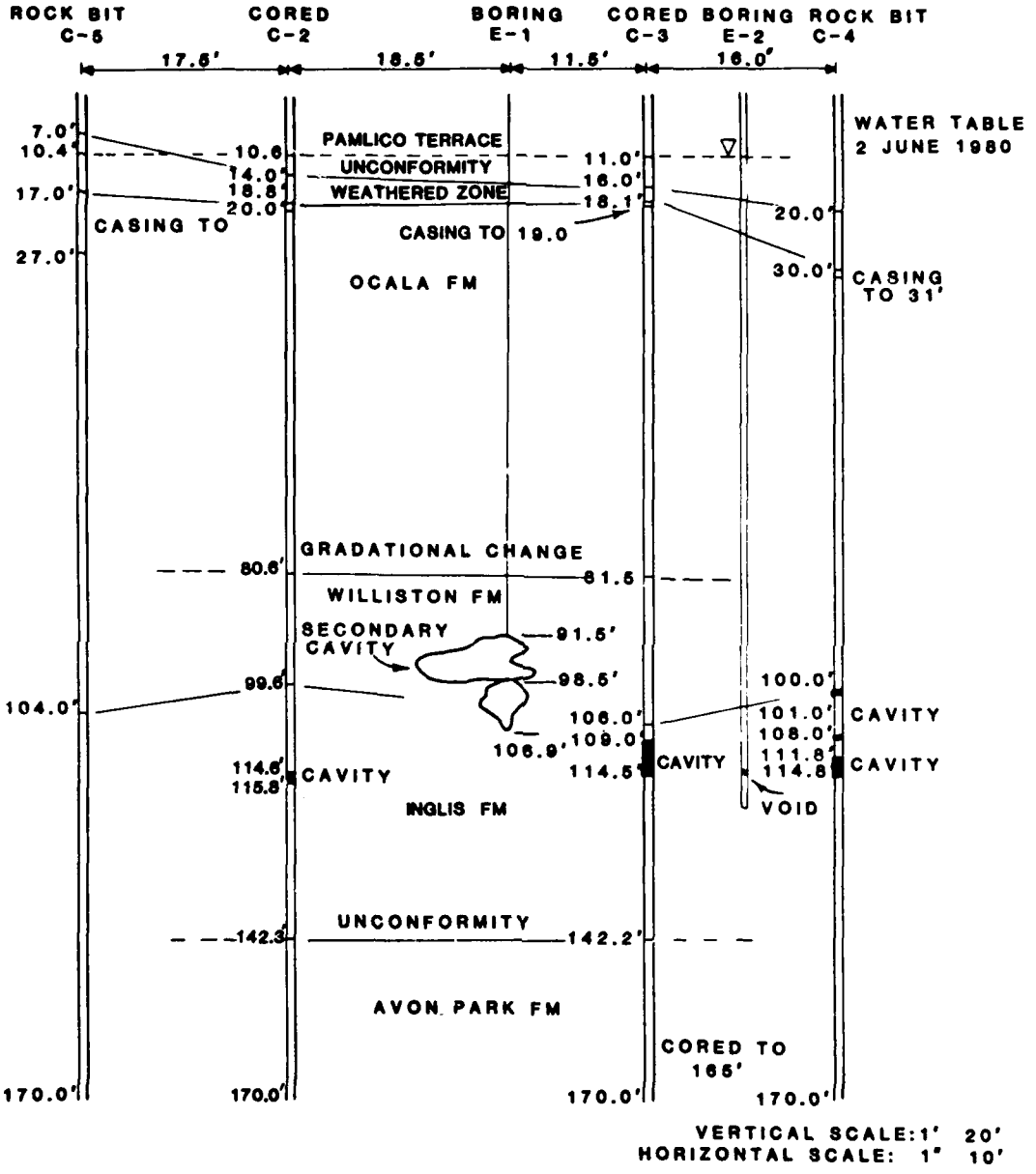

Figure 14. Cross section through borings C-2 to C-5 showing secondary cavity

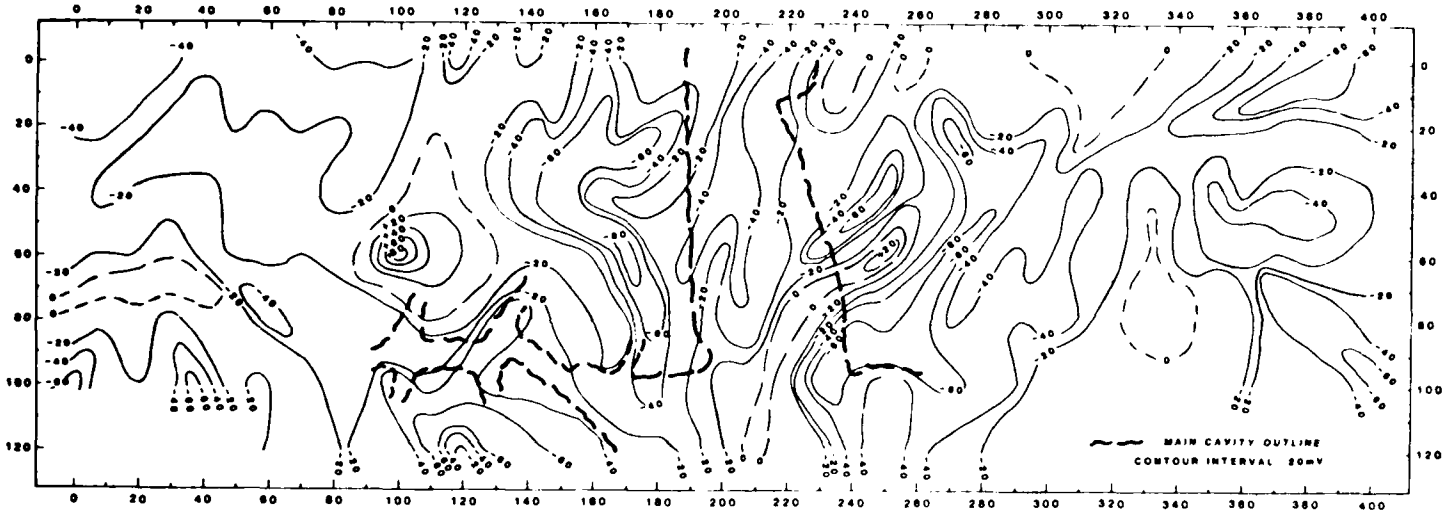

Figure 15. Contour plot of surface self-potential field above main and secondary cavity features, Manatee Springs test site

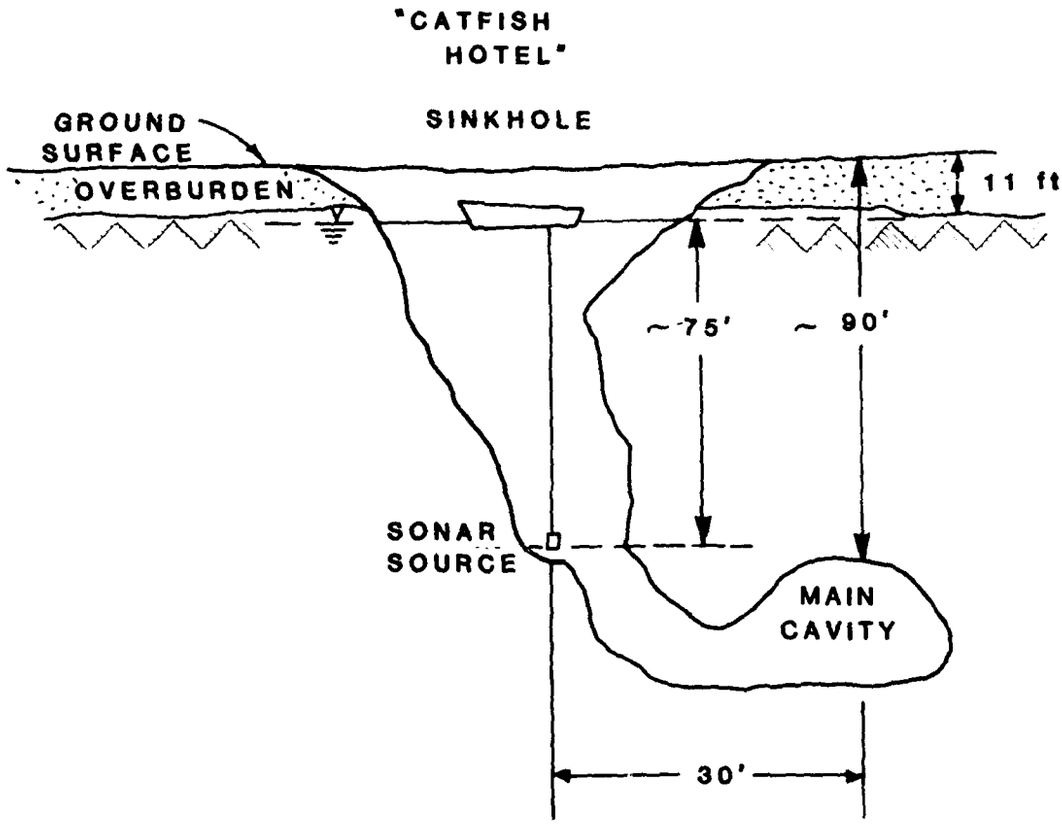

Figure 16. Cross section showing sonar source location in sinkhole communicating with main cavity system

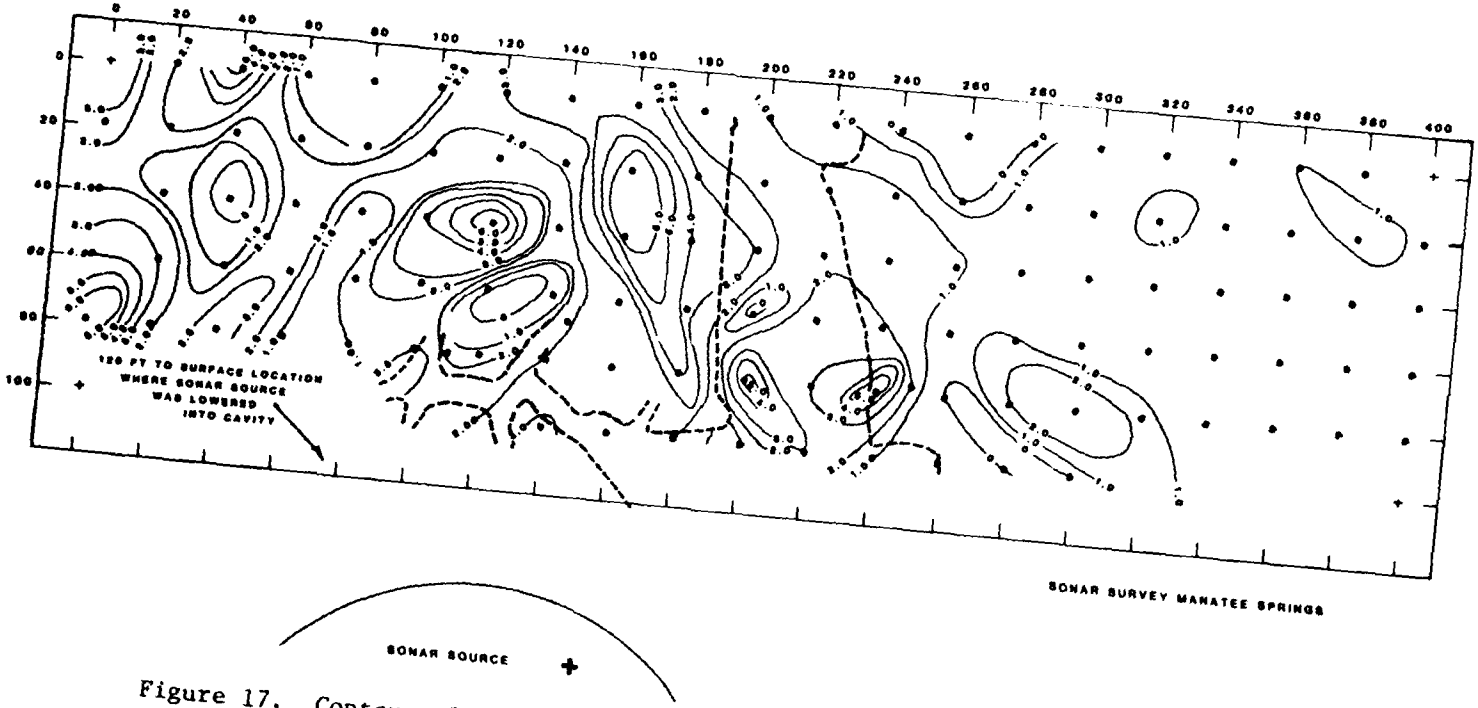

Figure 17. Contour plot of sonar signal magnitude in volts, peak-to-peak, recorded at Manatee Springs test site

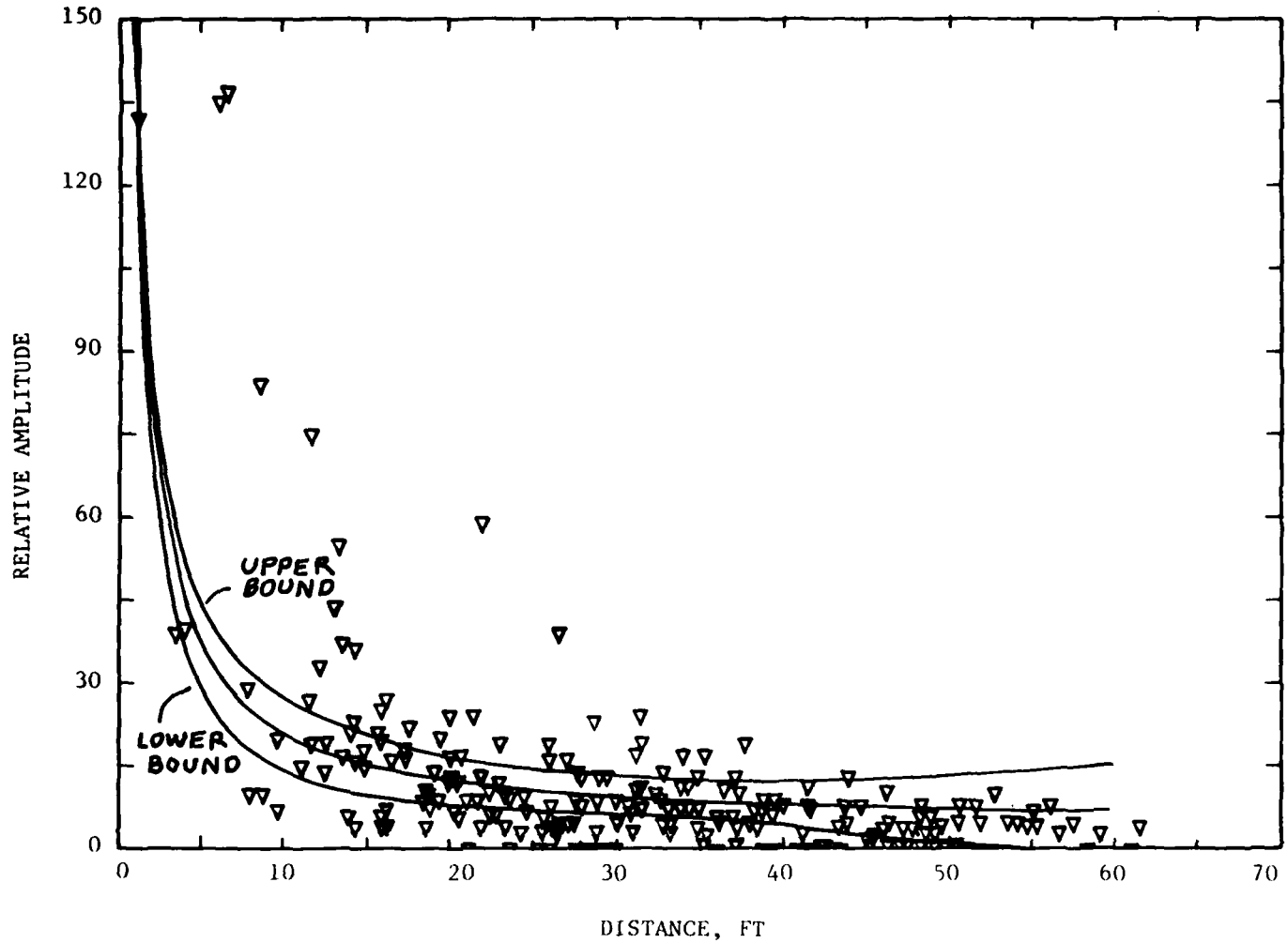

Figure 18. Acoustic signal attenuation versus range from the source, survey area 1, Medford Cave

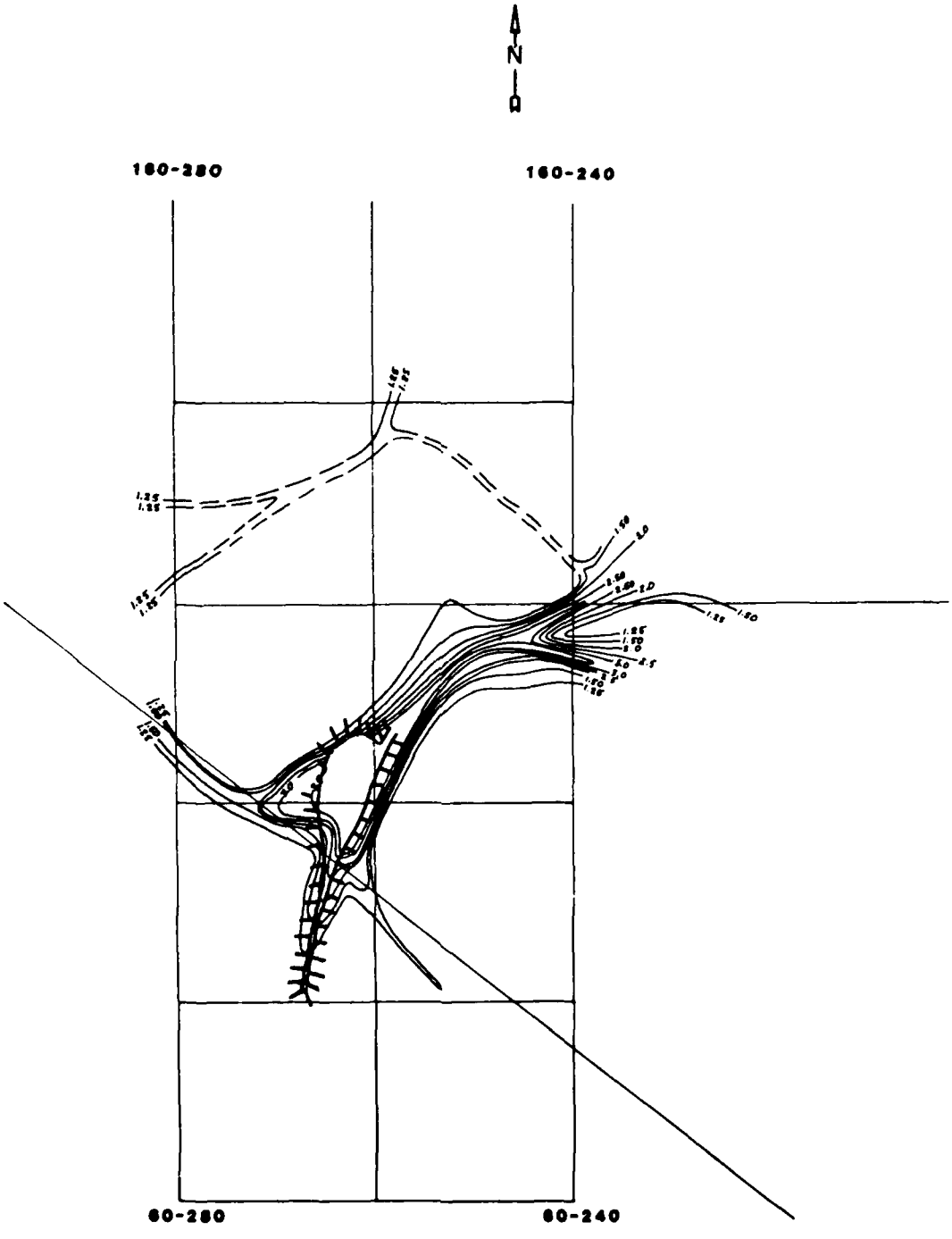

Figure 19. Attenuation normalized acoustic contour plot for test area 1, Medford Cave

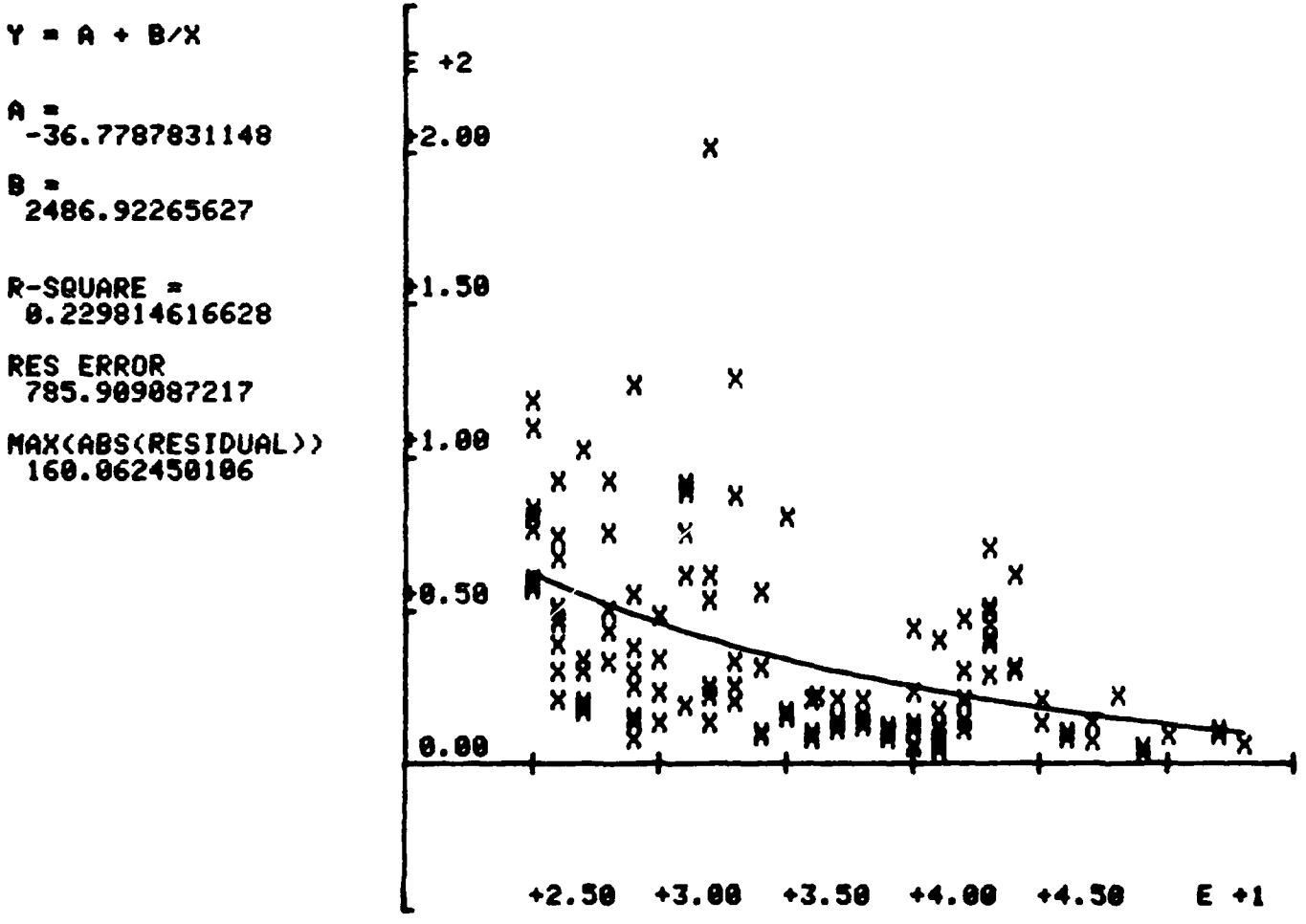

Figure 20. Acoustic signal attenuation versus range plot for test area 2, Medford Cave test site

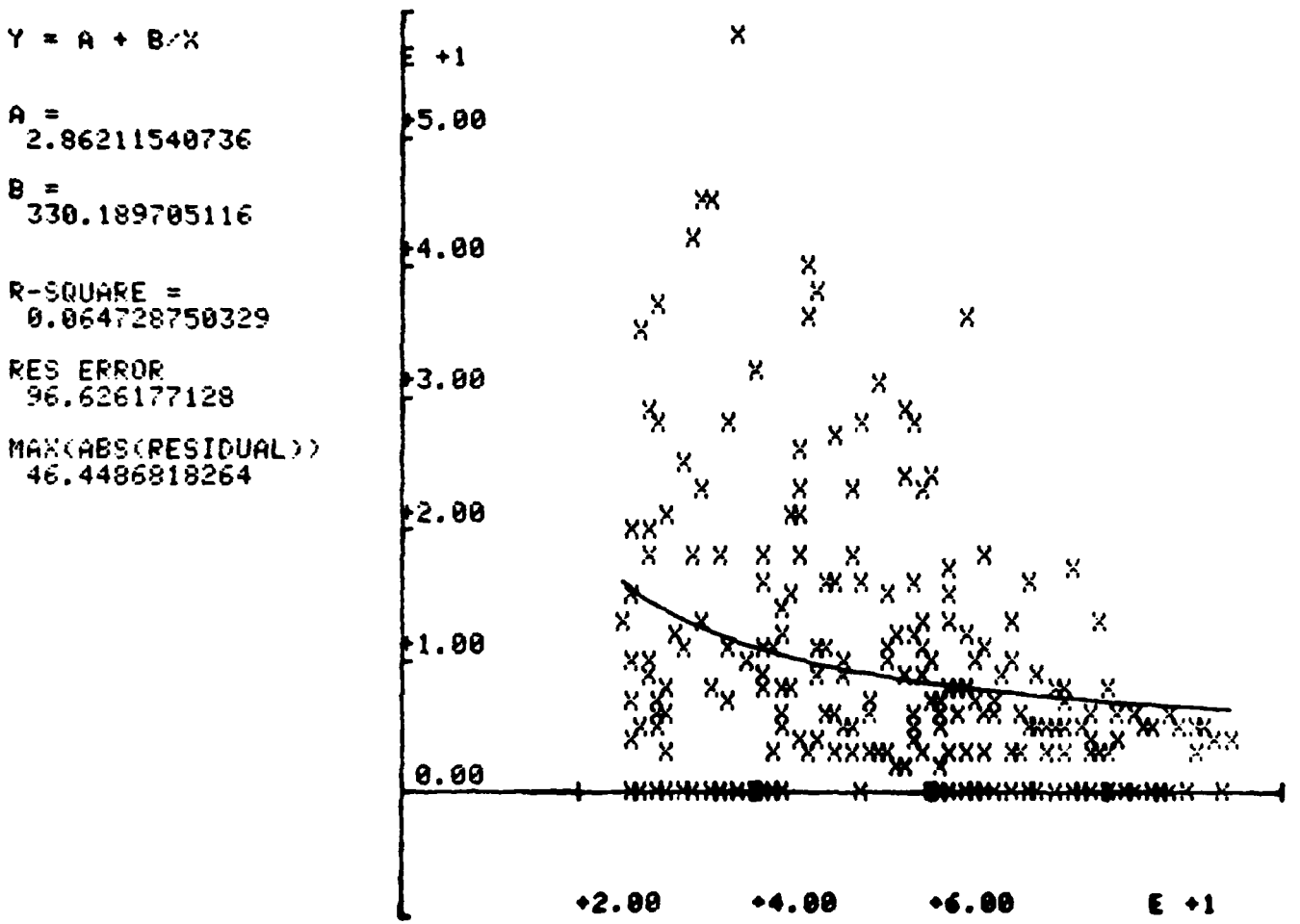

Figure 21. Acoustic signal attenuation versus range plot for test area 3, Medford Cave test site

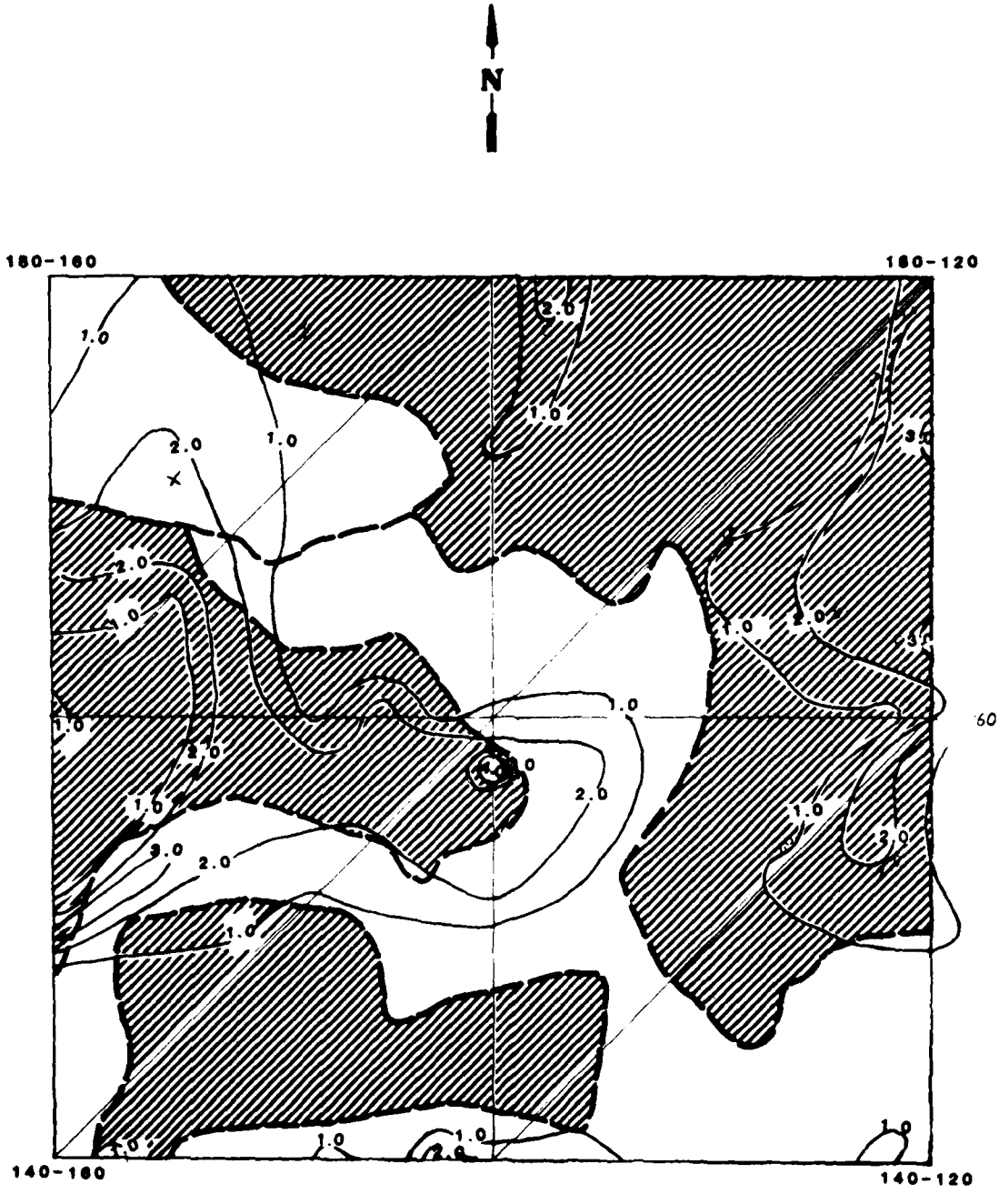

Figure 22. Attenuation-normalized acoustic contour plot for test area 2, Medford Cave test site

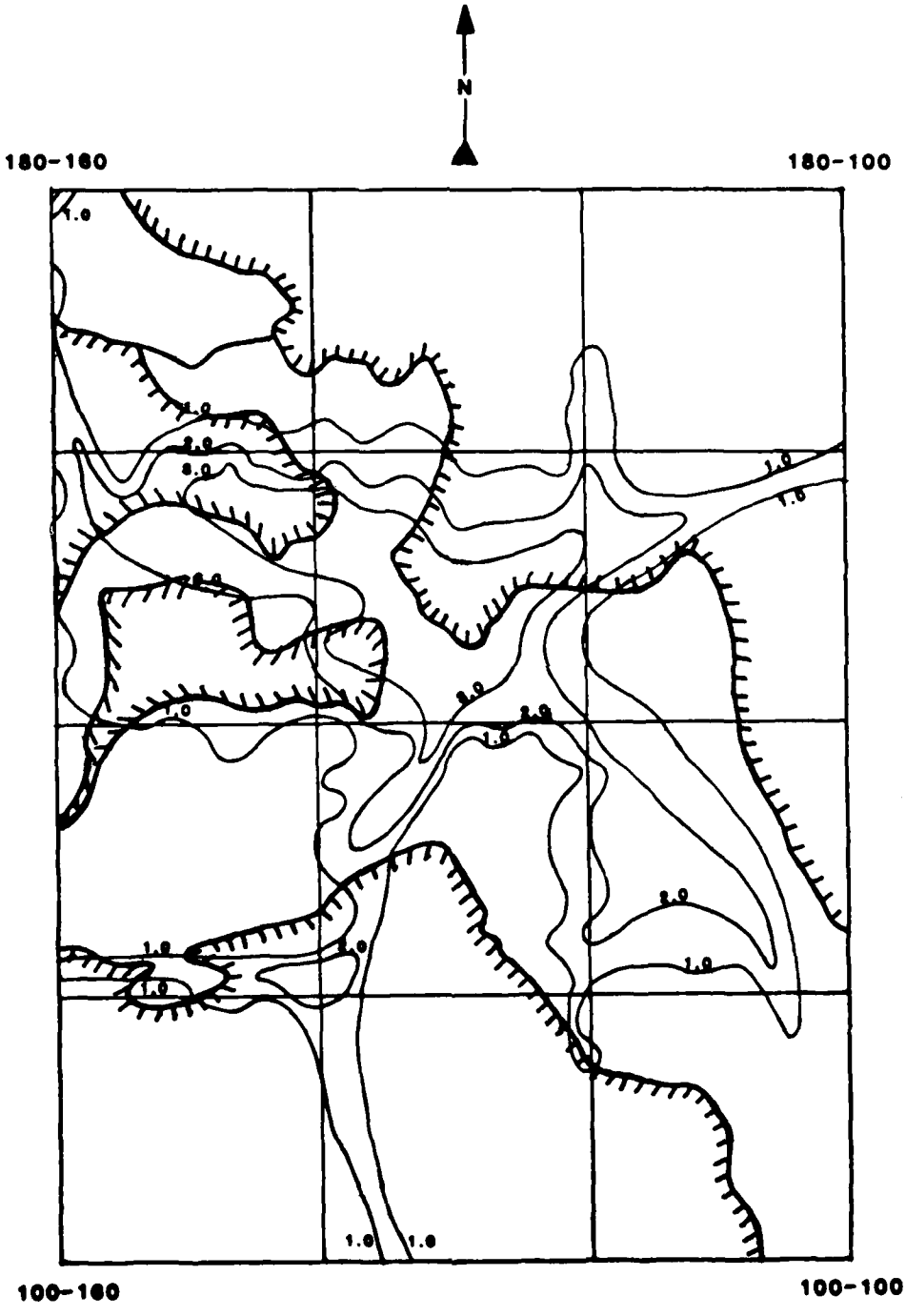

Figure 23. Attenuation normalized acoustic contour plot for test area 3, Medford Cave test site

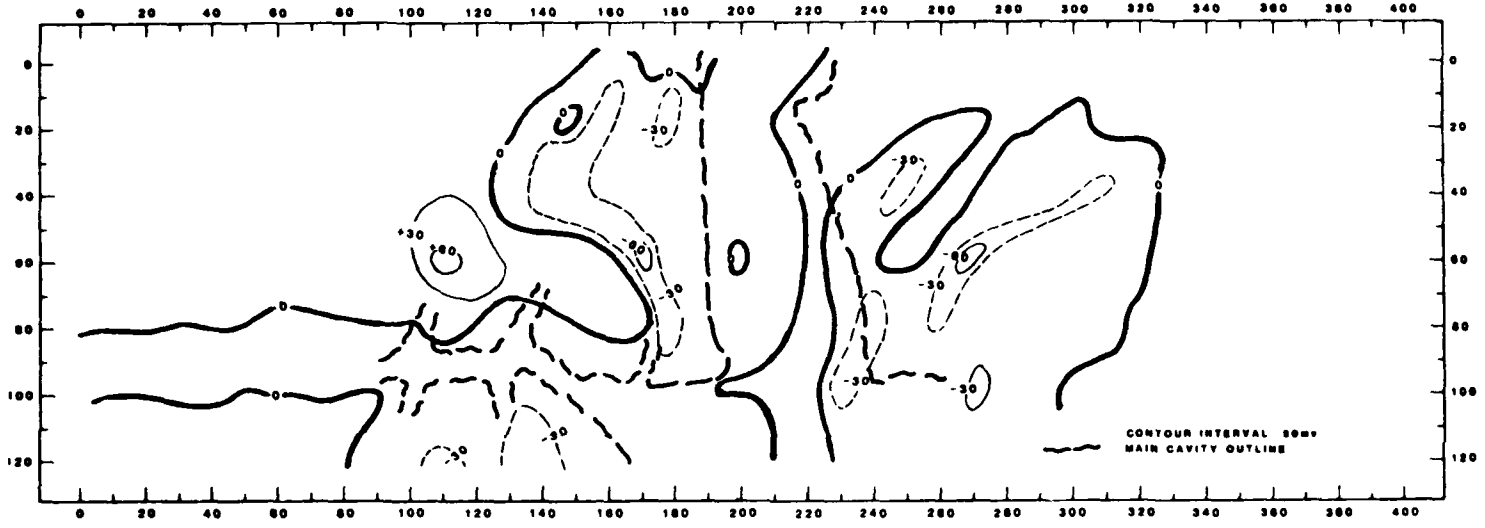

Figure 24. Self-potential contour map with regional mean SP value (-25 mv) removed

In accordance with letter from DAEN-RDC, DAEN-ASI dated 22 July 1977, Subject: Facsimile Catalog Cards for Laboratory Technical Publications, a facsimile catalog card in Library of Congress MARC format is reproduced below.

Cooper, Stafford S.
Cavity detection and delineation research : Report 3 : Acoustic resonance and self-potential applications : Medford Cave and Manatee Springs sites, Florida / by Stafford S. Cooper (Geotechnical Laboratory, U.S. Army Engineer Waterways Experiment Station). -- Vicksburg, Miss. : The Station ; Springfield, Va. : available from NTIS, 1983.
21, [39] p. : ill. ; 27 cm. -- (Technical report ; GL-83-1, Report 3)
Cover title.
"May 1983."
"Prepared for Office, Chief of Engineers, U.S. Army under CWIS Work Unit 31150."
Bibliography: p. 21.

1. Geophysical research. 2. Manatee Springs (Fla.). 3. Medford Cave (Fla.). 4. Sonar. 5. Springs--Florida. I. United States. Army. Corps of Engineers. Office of

Cooper, Stafford S.
Cavity detection and delineation research : ... 1983.
(Card 2)

the Chief of Engineers. II. U.S. Army Engineer Waterways Experiment Station. Geotechnical Laboratory. III. Title IV. Series: Technical report (U.S. Army Engineer Waterways Experiment Station) ; GL-83-1, Report 3.
TA7.W34 no.GL-83-1 Rept. 3


DATE
ILME